

Structural determinants of substrate recognition and catalysis by heparan sulfate sulfotransferases

Gesteira, Tarsis F; Marforio, Tainah; Mueller, Jonathan Wolf; Calvaresi, Matteo; Coulson-Thomas, Vivien Jane

DOI:

[10.1021/acscatal.1c03088](https://doi.org/10.1021/acscatal.1c03088)

License:

None: All rights reserved

Document Version

Peer reviewed version

Citation for published version (Harvard):

Gesteira, TF, Marforio, T, Mueller, JW, Calvaresi, M & Coulson-Thomas, VJ 2021, 'Structural determinants of substrate recognition and catalysis by heparan sulfate sulfotransferases', *ACS Catalysis*, vol. 11, no. 17, pp. 10974–10987. <https://doi.org/10.1021/acscatal.1c03088>

[Link to publication on Research at Birmingham portal](#)

Publisher Rights Statement:

This document is the Accepted Manuscript version of a Published Work that appeared in final form in *ACS Catalysis*, copyright © American Chemical Society after peer review and technical editing by the publisher. To access the final edited and published work see: <https://doi.org/10.1021/acscatal.1c03088>

General rights

Unless a licence is specified above, all rights (including copyright and moral rights) in this document are retained by the authors and/or the copyright holders. The express permission of the copyright holder must be obtained for any use of this material other than for purposes permitted by law.

- Users may freely distribute the URL that is used to identify this publication.
- Users may download and/or print one copy of the publication from the University of Birmingham research portal for the purpose of private study or non-commercial research.
- User may use extracts from the document in line with the concept of 'fair dealing' under the Copyright, Designs and Patents Act 1988 (?)
- Users may not further distribute the material nor use it for the purposes of commercial gain.

Where a licence is displayed above, please note the terms and conditions of the licence govern your use of this document.

When citing, please reference the published version.

Take down policy

While the University of Birmingham exercises care and attention in making items available there are rare occasions when an item has been uploaded in error or has been deemed to be commercially or otherwise sensitive.

If you believe that this is the case for this document, please contact UBIRA@lists.bham.ac.uk providing details and we will remove access to the work immediately and investigate.

This document is confidential and is proprietary to the American Chemical Society and its authors. Do not copy or disclose without written permission. If you have received this item in error, notify the sender and delete all copies.

Structural determinants of substrate recognition and catalysis by heparan sulfate sulfotransferases

Journal:	<i>ACS Catalysis</i>
Manuscript ID	cs-2021-03088d.R1
Manuscript Type:	Article
Date Submitted by the Author:	n/a
Complete List of Authors:	Gesteira, Tarsis; University of Houston College of Optometry, Optometry Marforio, Tainah Dorina; University of Bologna, Chemistry Department, "Giacomo Ciamician" Mueller, Jonathan; University of Birmingham Institute of Metabolism and Systems Research Calvaresi, Matteo; Università degli Studi di Bologna, Dipartimento di Chimica Coulson-Thomas, Vivien; University of Houston College of Optometry, Optometry

SCHOLARONE™
Manuscripts

Structural determinants of substrate recognition and catalysis by heparan sulfate sulfotransferases

Tarsis Ferreira Gesteira^{§*}, Tainah Dorina Marforio[‡], Jonathan Wolf Mueller[†], Matteo Calvaresi[‡] and Vivien Jane Coulson-Thomas[§]

[§]College of Optometry, University of Houston, Houston, Texas 77004, United States

[‡] Dipartimento di Chimica “Giacomo Ciamician”, Università di Bologna, Bologna 40126, Italy

[†]Institute of Metabolism and Systems Research, University of Birmingham, Birmingham B15 2TQ, UK.

ABSTRACT

Heparan sulfate (HS) and heparin contain imprinted “sulfation codes”, which dictate their diverse physiological and pathological functions. A group of orchestrated biosynthetic enzymes cooperate in polymerizing and modifying HS chains. The biotechnological development of enzymes that can recreate this sulfation pattern on synthetic heparin is challenging, primarily due to the paucity of quantitative data for sulfotransferase enzymes. Herein, we identified critical structural characteristics that determine substrate specificity and shed light on the catalytic mechanism of sugar sulfation of two HS sulfotransferases, 2-O-sulfotransferase (HS2ST) and 6-O-sulfotransferase (HS6ST). Two sets of molecular clamps in HS2ST recognize appropriate substrates; these clamps flank the acceptor binding site on opposite sides. The hexuronic epimers, and not their puckers, have a critical influence on HS2ST selectivity. In contrast, HS6ST recognizes a broader range of substrates. **This promiscuity is granted by a conserved tryptophan residue, W210, that positions the acceptor within the active site for catalysis by means of strong electrostatic interactions.** Lysines K131 and K132 act in concert with a second tryptophan, W153, shedding water molecules from within the active site, thus, providing HS6ST with a binding preference towards 2-O-sulfated substrates. **QM/MM calculations** provided valuable mechanistic insights into the catalytic process, identifying the sulfation process for both HS2ST and HS6ST

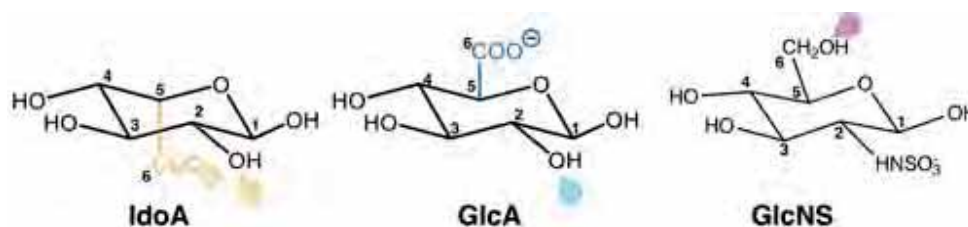
follows a S_N2 -like mechanism. Taken together, our findings reveal the molecular basis of how these enzymes recognize different substrates and catalyse sugar sulfation, enabling the generation of enzymes that could create specific heparin epitopes.

KEYWORDS

Heparin, glycosaminoglycan biosynthesis, sulfotransferase, sulfation, HS2ST, HS6ST, sugar ring-puckering, active-site solvation.

Introduction

Heparan sulfate (HS) and heparin, complex unbranched sulfated polysaccharides, are both ~~part of a class of molecules named~~ glycosaminoglycans (GAGs), consisting of a repeating disaccharide unit formed of glucosamine (GlcN) and glucuronic acid (GlcA)/iduronic acid (IdoA) residues.¹ HS is ubiquitously found in all cells and tissues and plays various biological roles in embryonic development, as well as in extracellular signaling, while heparin is expressed primarily in mast cells¹⁻³ and plays an important role in coagulation. Heparin is widely used in the medical field as an anticoagulant, with a global turnover of more than US\$ 6 billion in 2018.⁴ HS and heparin share the same biosynthetic pathway and mainly differ in the degree of chain sulfation; 80% of heparin is sulfated while ~50% of the HS chain is unmodified.⁵ During the polymerization of these GAGs, a series of non-template driven enzyme-catalyzed modifications take place.⁶⁻⁸ These include cleavage of the acetyl group from GlcNAc and concomitant N-sulfation by the bifunctional enzyme family of N-deacetylases/N-sulfotransferases (NDST isoforms NDST1-4)⁹ forming N-sulfoglucosamine (GlcNS). Glucuronyl C5-epimerase then converts GlcA (D-gluronic) to IdoA (L-iduronic).¹⁰ A final step is the addition of one or more sulfate groups; carried out by HS 2-, 3-, and 6-O-sulfotransferases (HS2ST, HS3ST and HS6ST, respectively).¹¹

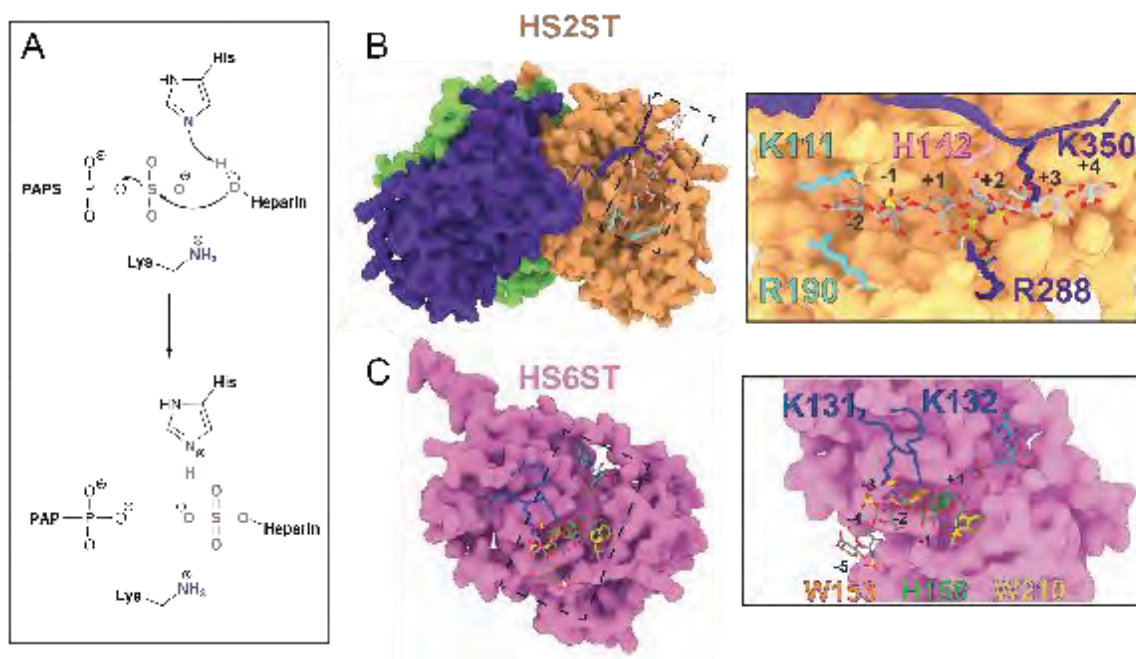


Scheme 1. Schematic representation of IdoA, GlcA and GlcNS monosaccharides. The C₅ centres of the epimers IdoA and GlcA are coloured in orange and blue, respectively. Drops (orange/blue for HS2ST and purple for HS6ST) point towards the sulfation sites.

1
2
3
4
5
6
7
8
9
10
11
12
13
14
15
16
17
18
19
20
21
22
23
24
25
26
27
28
29
30
31
32
33
34
35
36
37
38
39
40
41
42
43
44
45
46
47
48
49
50
51
52
53
54
55
56
57
58
59
60

These Golgi sulfotransferases are responsible for transferring the sulfate group from the cofactor molecule PAPS (3'-phosphoadenosine-5'-phosphosulfate) to a specific position of the acceptor unit, specifically: HS2ST sulfates the 2-OH position of GlcA/IdoA, HS6ST the 6-OH position of GlcNS (Scheme 1) and HS3ST the 3-OH position of GlcNS. The density and exact position of sulfate groups represent specific binding motifs for other biomolecules and, hence, is of paramount importance for the physiological functions of GAGs. Specifically, highly sulfated “patches” are often flanked by less sulfated regions within the HS/heparin chain.¹²⁻¹⁴ A significant body of work has shown that these sulfation patterns within the polysaccharide chain dictate their physiological functions.^{13, 15-21}

Sulfation at the 2 and 6 positions are functionally linked, since genetic²² and biochemical²³ inhibition of HS2ST sulfotransferase activity cause an increase in 6-O-sulfation, compensating for the loss of 2-O-sulfation. Since a functional link has been shown to exist between HS2ST and HS6ST, we focused on these two enzymes in this study (Figure 1). A single HS2ST isoform has been identified to date in humans which may play an important regulatory role in the biosynthetic process of GAGs.²⁴ Moreover, HS2ST *null* knockout mice display significant developmental abnormalities that lead to death of the early fetus, presenting bilateral renal agenesis and defects in the eyes and skeleton.^{25, 26}



1
2
3 **Figure 1.** Representation of HS2ST and HS6ST. (A) General ~~proposed~~ catalytic mechanism
4 exerted by HS2ST and HS6ST. (B) Surface representation of HS2ST trimmer. Each monomer
5 represented with a unique color. Insert highlights glycan clamps (K111/R190 in cyan and
6 R288/K350' in purple), and the H142 catalytic base. (C) Surface representation of HS6ST
7 monomer. Insert highlights W153 and W210 near the active site, catalytic H153 and the loop
8 containing the K131/K132 pair. The numbers indicate the position of the ~~saccharides~~
9 the acceptor unit.
10
11
12
13
14
15
16

17 HS2ST preferentially sulfates the C2 position of the hexuronic epimer IdoA, with a **much**
18 **lower sulfation activity** towards GlcA, specifically, HS2ST has a 2.5-fold preference towards IdoA
19 substrates.^{25, 27} The **next modification** occurs at the 6-position of the glucosamine residue by
20 HS6ST and this sulfation is critical for conferring antithrombin activity to heparin.²⁸ The HS6ST
21 isoforms HS6ST-1, -2, and -3 and an additional alternatively spliced isoform, HS6ST-2S, have
22 been identified in mammals.²⁹ There is evidence that all HS6ST isoforms exhibit a substrate
23 preference for a negatively charged sugar (a uronic acid residue) neighboring a N-
24 sulfoglucosamine.^{12, 30, 31} **The crystal structure of zebrafish HS6ST isoform 3 has recently been**
25 **solved revealing a unique orientation of HS binding.**¹⁴ In 2-O-, 3-O- and N-sulfotransferases, the
26 saccharide binds perpendicularly to the sulfate donor PAPS in an open cleft. **In contrast,** a recent
27 crystallographic study revealed that for HS6ST, this cleft is closed by a coil that shallows the
28 binding cleft, suggesting that glycan binding may exert some modulatory function by burying
29 PAPS within the active site ensuring **its proper** placement.¹⁴ This unusual topology is thought to
30 explain HS6ST promiscuity towards different substrates, ~~and the different HS6ST isoforms appear~~
31 ~~to have similar reactivity towards diverse substrates.~~³²
32
33
34
35
36
37
38
39
40
41
42

43 HS2ST and HS6ST are central enzymes in HS/heparin biosynthesis, and a precise molecular
44 understanding of the protein:GAG interactions is vital to understanding the mechanisms that
45 control HS and heparin sulfation. By synergistically exploiting *in silico* and *in vitro* approaches,
46 we hereby identified structural characteristics that determine substrate specificity for HS2ST and
47 HS6ST and deciphered the mechanism by which these enzymes sulfate their substrates. In
48 particular, we elucidate the contribution and the role of individual residues within the active site
49 to substrate recognition and catalysis for HS2ST and HS6ST. The structural framework presented
50 here opens new avenues for designing substrate-specific sulfotransferases and for building a
51
52
53
54
55
56
57
58
59
60

platform that would enable cost-effective synthesis of diverse HS oligosaccharides with different sulfation patterns towards heparin-based therapeutics.

Methods

The Methods section is provided within the Supporting Information file and consists of: i) system setup and Molecular Dynamic (MD) simulations, ii) the Molecular-Mechanics Generalized-Born Surface Area (MM-GBSA) method, iii) multiple sequence alignment, iv) enzymatic assays, v) Metadynamics simulations for sugar puckering and water coordination, vi) QM/MM setup and ONIOM calculations, vii) ring puckering analysis, viii) interaction fingerprint analysis, and ix) Grid Inhomogeneous Solvation Theory (GIST) analysis.

Results and Discussion

Structural motions of the HS2ST enzyme bound to crystallographic substrate.

Our work starts with the analysis of HS2ST crystal structure (PDB ID 4NDZ), which consists of a Trimer that binds the glycan acceptor substrate in the 4C_1 -IdoA conformation within a groove formed by one subunit complemented by a C-terminal beta-strand that is swapped over from a neighboring subunit (Figure 1). We carried out extensive 2 microsecond MD simulations of i) the substrate- and PAPS-free apo HS2ST homotrimer (HS2ST_{apo}), ii) the HS2ST homotrimer complexed to PAPS and GlcA₊₅-GlcNAc₊₄-GlcA₊₃-GlcNS₊₂- **4C_1 -IdoA₊₁**-GlcNS₋₁-GlcA₋₂ (PDB ID: 4NDZ)²⁷, hereafter referred to as HS2ST: 4C_1 IdoA, and iii) the HS2ST homotrimer bound to PAPS and GlcA₊₅-GlcNAc₊₄-GlcA₊₃-GlcNS₊₂- **4C_1 -GlcA₊₁**-GlcNS₋₁-GlcA₋₂ (where we manually located a glucuronic acid at the catalytic position), hereafter referred to as HS2ST: 4C_1 -GlcA. The saccharide unit that undergoes sulfation is in position “+1” and is indicated in bold. Since the simulated HS2ST is a homotrimer, all the results reported herein are referred to as the averaged results of a triplicate of two runs. Upon examining HS2ST:glycan simulations, we identified for the first time a group of positively charged residues forming molecular clamps in both the HS2ST: 4C_1 -GlcA and HS2ST: 4C_1 -IdoA complexes that are “open” or “closed” in order to stably position the negatively charged hexasaccharide substrates within the active site. Specifically, these molecular clamps are formed by amino acid residues K111/R190 and R288/K350’ (“prime” - because it is from the C-terminus of the adjacent monomer). The

1
2
3
4
5
6
7
8
9
10
11
12
13
14
15
16
17
18
19
20
21
22
23
24
25
26
27
28
29
30
31
32
33
34
35
36
37
38
39
40
41
42
43
44
45
46
47
48
49
50
51
52
53
54
55
56
57
58
59
60

K111/R190 clamp (in cyan in Figure 1B) interacts with the substrate hexasaccharide at the +4 position, while R288/K350' flanks the acceptor unit (at position +1) and at GlcNS2S₊₂ (in purple in Figure 1B). Intriguingly, we found that these residues are highly conserved among vertebrate HS2ST enzymes (Figure S1), suggesting that they play a crucial role in positioning the ligand precisely within the active site. To follow the movement of the clamps during the MD simulations, the center of mass of both LYS/ARG residue pairs was tracked for each clamp. For HS2ST_{apo}, the average distance between the K111/R190 pair was 18 Å (Figure 2A, left panel). In the HS2ST:⁴C₁-GlcA and HS2ST:⁴C₁-IdoA complexes, however, the average clamp distance was reduced to around 13 Å (Figure 2A, center and right panels), reinforcing the hypothesis that the K111/R190 clamp closes upon binding of the substrate, requiring the presence of a high motility loop from residues 180 to 197.³³

The opening of the R288/K350' dyad varied significantly between the HS2ST:⁴C₁-GlcA and HS2ST:⁴C₁-IdoA simulations (Figure 2A, center and right panels). Specifically, the average opening of R288/K350' for HS2ST:⁴C₁-IdoA was stable at ~10.5 Å, while for HS2ST:⁴C₁-GlcA it fluctuated between ~7 and 12 Å. The analysis of dynamic cross-correlation (DCC) plots, which enables qualitative measurements of the interdependent enzyme dynamic coupling (Figure S3 and Discussion S1), show that the simple substitution of the acceptor unit from GlcA to IdoA has a substantial effect on HS2ST motility.

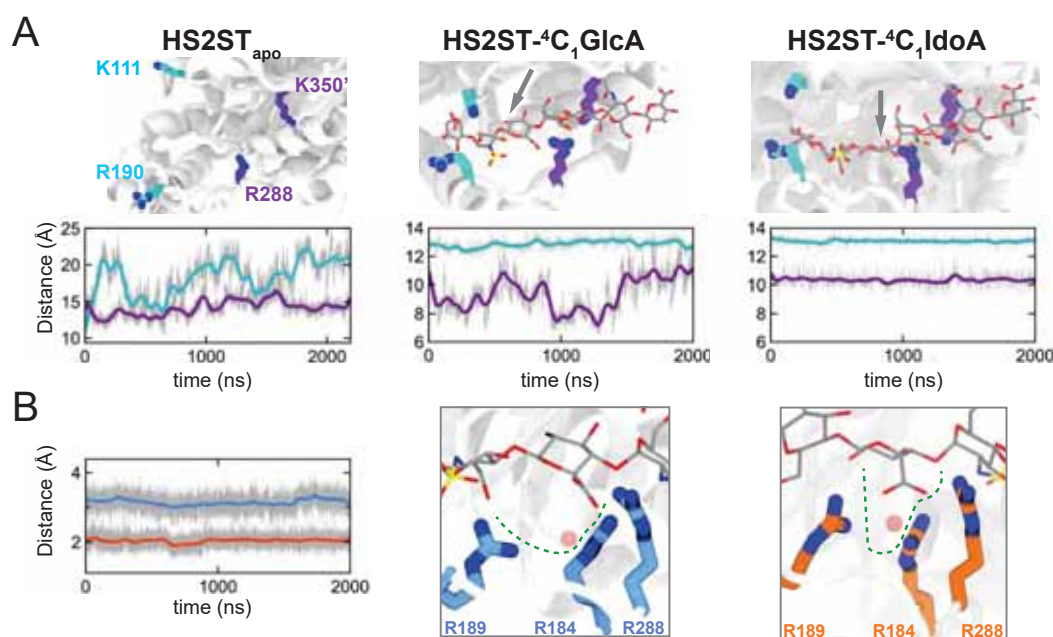


Figure 2. Uronic acid epimers binding to HS2ST. **(A)** Clamp pairs center of mass distances during simulations with the apoprotein, HS2ST:⁴C₁-GlcA or HS2ST:⁴C₁-IdoA. **(B)** Center of mass (pink sphere) distance of arginine triad R184/R189/R288 to the C6 atom of either IdoA (in orange) or GlcA (in blue).

Affinity of the HS2ST sulfotransferase for GlcA and IdoA at pucker ⁴C₁ as in the co-crystal structure.

The substrate binding was affected by enzyme motility and during our HS2ST:⁴C₁-GlcA MD simulations for two out of three subunits of HS2ST, we observed the dissociation of the oligosaccharide ligand from the enzyme binding pocket (RMSD values are reported in Figure S4). We quantified the binding free energy of the HS2ST:glycan systems by the MM-GBSA calculation means (see Supporting Information, Methods section). These analyses show that the ⁴C₁-IdoA-containing ligand binds to HS2ST at an average ΔG of -88.5 ± 1.2 kcal/mol, while the formation of the HS2ST:⁴C₁-GlcA complex gains -76.8 ± 2.5 kcal/mol (Table S2).

In order to understand differences in binding affinity, we analyzed the surrounding environment of HS2ST:⁴C₁-GlcA and HS2ST:⁴C₁-IdoA ligand binding pockets during simulations. Consistent with previous experimental data,^{27, 34, 35} we identified a positively charged fork formed by three arginine residues, R184, R189 and R288, that anchors the ligand at the sulfate acceptor unit (⁴C₁-GlcA₊₁ and ⁴C₁-IdoA₊₁) (Figure 2B). The distance between the C6-acceptor unit of either the HS2ST:⁴C₁-GlcA complex (Figure 2B, with arginines depicted as blue carbons) or the HS2ST:⁴C₁-IdoA complex (Figure 2B, with arginines depicted as orange carbons) and the center of mass of the fork was also tracked over the simulation time. The distance observed was 3.2 Å on average for ⁴C₁-GlcA₊₁ (blue line) and 2.4 Å on average for ⁴C₁-IdoA₊₁ (orange line), indicating that the arginine fork provided an efficient electrostatic trap for the negatively charged carboxylated C₆ group of the acceptor IdoA residue, while the “in plane” C₆OO⁻ of the GlcA acceptor does not fit properly within the fork trap.

To further quantify the contribution of the key amino acids (K111/R190 and R288/K350'clamps and R184/R189/R288 fork) to overall binding, MM-GBSA per-residue energy decomposition analysis was performed on HS2ST:⁴C₁-GlcA and HS2ST:⁴C₁-IdoA (Figure S5 and Table S3). The lysine of the K111/R190 clamp contributes by -3.8 ± 0.1 kcal/mol to the binding of the ⁴C₁-IdoA-containing substrate, and by -2.3 ± 0.0 kcal/mol for HS2ST:⁴C₁-GlcA, while R190 displays a slight

1
2
3
4 preference towards HS2ST:⁴C₁-IdoA (-5.8±0.8 and -1.9±0.4 kcal/mol, respectively). The
5 contribution of R288 is high for both complexes, being -11.8±0.8 and -12.1±0.6 kcal/mol for
6 HS2ST:⁴C₁-GlcA and HS2ST:⁴C₁-IdoA, respectively. The last residue, K350', located at the
7 adjacent monomer, contributes by -18.7±1.6 in HS2ST:⁴C₁-IdoA and -5.8±2.0 kcal/mol in
8 HS2ST:⁴C₁-GlcA simulations. The three arginine residues that form the fork (R184, R189 and
9 R288) contribute together to a total binding of -20.5±1.5 kcal/mol for HS2ST:⁴C₁-GlcA, and -
10 24.0±2.1 kcal/mol for HS2ST:⁴C₁-IdoA. These contributions suggest that the three residues play a
11 fundamental role in binding the substrate, especially R288, which was identified in the two
12 structural motifs responsible for binding the substrate (the R288/K350' clamp and the
13 R184/R189/R288 fork). It has been reported in the literature that mutating R189 to alanine
14 (R189A) causes a loss of the enzyme preference for IdoA as an acceptor,³³ and that
15 HS2ST(R189A) is capable of sulfating GlcA to a higher extent when compared to the wild-type
16 enzyme.²⁷ To date, there are no reports on whether it is the charge and/or steric hindrance of R189
17 side-chains that govern these two observed phenomena.^{27, 33} Therefore we performed an *in vitro*
18 enzymatic assay on wild-type HS2ST, and, in order to evaluate the steric effect of a large but
19 neutral amino acid on the enzyme ability to sulfate the acceptor, we generated a mutant harboring
20 an arginine to leucine mutation (R189L), and a second mutant (R189K) was generated to evaluate
21 the effect of a different positively charged residue. The R189A mutant was expressed as in Liu et
22 al³⁴ to coherently enable a comparison of our results. The WT and mutated enzymes were
23 incubated with (GlcNS-GlcA)₃ polysaccharide substrates, and the products produced analyzed by
24 strong anion exchange high performance liquid chromatography (HPLC), as described in
25 Supporting methods. The wild-type HS2ST enzyme presented 92% less activity towards [-GlcNS-
26 GlcA-]₃ compared to [-GlcNS-IdoA-]₃ (Figure S6). Similarly, the mutants R189K and R189L
27 exhibited less activity (<10%) towards (GlcNS-GlcA)₃, while R189A maintained 100% activity
28 towards (GlcNS-GlcA)₃. Thus, our experimental data suggests there is a balance between the
29 charge and steric effect of the arginine sidechain, reinforcing the idea that the R189 charged
30 guanidinium moiety plays a crucial role in recognizing the hexuronic epimer. We also carried out
31 an *in-silico* investigation of R189A mutation, by performing a 2 μs MD simulation of
32 HS2ST(R189A):⁴C₁-GlcA. In this simulation, A189 did not obstruct the binding of GlcA within
33 the fork as did R189 (Figure S6A-B). Indeed, GlcA can enter the fork and bind to R184 and R288.
34 The contributions of R184 and R288 to ligand binding for HS2ST(R190A):⁴C₁-GlcA are -6.5±0.1
35
36
37
38
39
40
41
42
43
44
45
46
47
48
49
50
51
52
53
54
55
56
57
58
59
60

1
2
3 kcal/mol and -2.8 ± 0.5 kcal/mol respectively, suggesting that when abolishing R189, the other two
4 residues (R184 and R288) are not able to “recreate” the electrostatic fork to entrap the hexuronic
5 unit. Taken together, the experimental and computational data demonstrate that R189 plays a
6 critical role in defining HS2ST substrate specificity.
7
8

9
10 Based on per-residue decomposition analysis carried out on all the amino acids surrounding the
11 binding site, R80 also displays favorable and strong interactions with both HS2ST:⁴C₁-GlcA and
12 HS2ST:⁴C₁-IdoA (-10.8 ± 0.8 and -13.1 ± 0.7 kcal/mol, respectively). While the fork recognizes and
13 fits the carboxylated group of the hexuronic acid, R80 is responsible for recognizing the GlcN2S
14 unit at +2 position, reinforcing the hypothesis that N-sulfation is a prerequisite for 2-O-sulfation.³⁴
15 We can also observe distinctive ways in which the NREs of the polysaccharide substrates bind to
16 HS2ST in the HS2ST:⁴C₁-GlcA and HS2ST:⁴C₁-IdoA simulations. The observed contribution of
17 K354' towards substrate binding for HS2ST:⁴C₁-IdoA (-8.4 ± 2.1 kcal/mol) and HS2ST:⁴C₁-GlcA
18 (~ 0 kcal/mol) highlight the idea that contacts between the oligosaccharide NRE and the enzyme
19 are lost when the predominant epimer is GlcA, while when the glycan is IdoA these contacts are
20 retained.
21
22
23
24
25
26
27
28
29
30

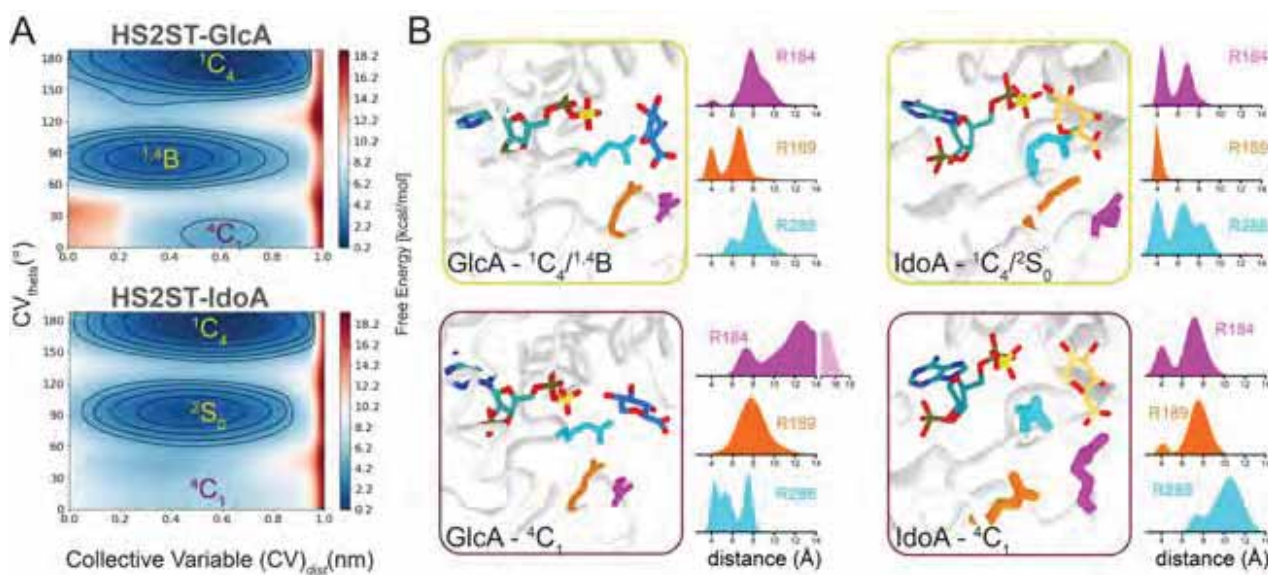
31 **HS2ST senses the conformation of uronic acid of its substrates.**

32
33 GlcA and IdoA epimers can adopt different conformations. For the majority of pyranoses,
34 including GlcA, the ⁴C₁ chair conformation is the only relevant conformation, since other
35 conformations require much higher energy.³⁶ However, IdoA shows a higher degree of
36 conformational flexibility. Indeed, all PDB entries (~ 100) containing IdoA that were
37 crystallographically solved at an atomic resolution of < 1.5 Å up until the time of this study
38 presented the uronic ring in the ¹C₄ chair conformation. In the recently crystallized HS2ST (PDB
39 ID: 4NDZ), the polysaccharide presents uronic acid in the ⁴C₁ conformation, an unusual pucker
40 for native GAGs. In fact, HS/heparin chains are composed of 30-250 disaccharides, and it is
41 reported that there is an increase in ¹C₄-IdoA within polysaccharides above 12 residues,^{37, 38}
42 reinforcing the hypothesis that real substrates comprise iduronic acid in the ¹C₄ conformation rather
43 than in the ⁴C₁ conformation. Since it is unlikely that HS2ST would induce such pyranoside ring
44 distortion, the observation of ⁴C₁-IdoA in the HS2ST crystal can be explained by the fact that the
45 polysaccharide used for crystallization is small.³⁹ In order to explore the free energy landscape for
46
47
48
49
50
51
52
53
54
55
56
57
58
59
60

HS2ST:IdoA and HS2ST:GlcA complexes along with the sugar conformations, we carried out well tempered metadynamics to bias different sugar puckers.

The resulting free energy surface (FES) for HS2ST:GlcA shows three wells associated with the 4C_1 , 1,4B and 1C_4 glucuronic acid (Figure 3A, top panel) and 4C_1 , 2S_0 and 1C_4 iduronic acid (Figure 3A, bottom panel) conformations. These minima are plotted as a Mercator projection of the Cremer-Pople sphere and expressed in terms of θ angle vs the distance between the acceptor oxygen and the PAPS sulfate (Figure 3A). Since Φ (O5–C1–O4–C4) and θ (C1–O4–C4–C5) dihedral angles dictate the orientation of the sugar ring in polysaccharides, the free energy surfaces of Φ/θ projections can be obtained as seen in Figure S7.

For GlcA, the lowest energy basins are 1,4B and 1C_4 while IdoA preferentially adopts a distorted conformation (2S_0) along with 1C_4 (180°) in the enzyme-substrate complexes. It is known that, in solution, IdoA has three distinguishable minima: the 4C_1 chair, the 2S_0 skew and the reverse 1C_4 chair; Spiwok et al. have calculated a free energy barrier of ~ 7 kcal/mol for the 4C_1 to 2S_0 transition in water.⁴⁰ In the HS2ST environment, the pucker minima profiles cover most of the Equatorial and Northern half of the pseudorotation cycle, with a barrier decreased to 5 kcal/mol between 1,4B



and 1C_4 .

Figure 3. Metadynamics of the HS2ST acceptor sugars. **(A)** Conformational FES (theta vs distance from PAPS) obtained for HS2ST:GlcA or HS2ST:IdoA. Each contour line of the diagram corresponds to 5 kcal/mol. **(B)** Distribution of key interactions in terms of the distances from the acceptor hexosamine to the arginines composing the fork to in the ${}^1C_4/{}^4C_1$ states (yellow and purple

1
2
3 outlines, respectively). The distance of the uronic acceptor heavy atoms to the guanidine group of
4 R184, R189 and R288 was calculated.
5
6

7
8 To verify the stability of HS2ST with the differently puckered ligand complexes, we carried out
9 2 μ s MD simulations of HS2ST:¹C₄-IdoA and HS2ST:¹C₄-GlcA (where we constrained the GlcA
10 to the improbable ¹C₄ conformation), and then we performed MM-GBSA computations. The total
11 binding free energies, reported in Table S2 and Figure S8, were -81.5 \pm 2.9 kcal/mol for HS2ST:¹C₄-
12 GlcA and -114.7 \pm 1.4 kcal/mol for HS2ST:¹C₄-IdoA. Interestingly, the computed binding affinity
13 is indicative of tighter binding of ¹C₄-IdoA respect to ⁴C₁-IdoA, reinforcing the idea that the
14 enzyme preferentially recognizes the natural occurring iduronic acid conformation. Thereafter, we
15 quantified the contribution of interface residues on the binding affinity of the substrate. For sake
16 of clarity, the per-residue decomposition results obtained for all the HS2ST:glycan systems are
17 summarized in Figure S5 and Table S3.
18
19

20
21 The three arginines (R184, R189, R288) have a pronounced preference for the ¹C₄-IdoA unit
22 (orange columns) in comparison to ⁴C₁-IdoA (blue columns), the less probable pucker for iduronic
23 acid. This is also verified for the other epimers, since the fork seems to bind preferably to ⁴C₁-
24 GlcA (green columns) rather than ¹C₄-GlcA (wine columns), an improbable conformation. The
25 fitting/unfitting of the carboxylated group of the acceptor unit (⁴C₁-IdoA/⁴C₁-GlcA) may provide
26 a plausible mechanistic explanation for the preference of this enzyme for IdoA over GlcA
27 containing substrates. We then examined the distribution of the distances of GlcA and IdoA
28 epimers within the arginine triad during the metadynamics simulations (Figure 3B). In the various
29 GlcA conformers, the pyranose ring could be distorted from ⁴C₁ and ^{1,4}B/¹S₃ to minimize clashes
30 with the recognizing arginine fork (R184, R189 and R288) (Figure 3B, yellow square in the left
31 panel). However, at this pucker the GlcA substrate is not in position for catalysis, as the GlcA O2
32 is distanced >5 Å from the PAPS sulfate (Figure 3B, left panel). When the acceptor GlcA is in the
33 ⁴C₁ conformation, it is not within a suitable distance to interact with R184/R189, and arginine fork
34 binding is improbable, despite it being equatorially oriented to receive the sulfate. Interestingly,
35 the ⁴C₁ pucker has a much more drastic effect on the IdoA interaction with R288 within the
36 arginine fork (Figure 3B, purple insert in the left panel). The sampled puckers have little effect on
37 IdoA acceptor orientation within the PAPS donor, an indication that these two variables are not
38 directly correlated. Taken together, our data suggest the steric/hydrogen bonding effect exerted by
39
40
41
42
43
44
45
46
47
48
49
50
51
52
53
54
55
56
57
58
59
60

1
2
3 R184/R189/R288 over the equatorial exocyclic oxygen atoms is a determinant of the observed
4 HS2ST preference for IdoA over GlcA moieties.
5
6

7 **How does the uronic acid conformation influence HS2ST catalysis?**

9
10 In order to further assess if and how the uronic pucker influences the sulfate transfer by HS2ST,
11 we modelled the reaction mechanism for the following acceptor conformations: the 4C_1 , 2S_0 and
12 1C_4 conformers for IdoA, and 4C_1 and 1C_4 for GlcA. The starting point for QM/MM calculations
13 corresponding to the NAC (Near Attack Conformation) structure was extracted from the MD
14 simulation (Figure S2). Figure 4 shows a schematic representation of the reaction mechanism and
15 the activation barriers (ΔG^\ddagger) and reaction energies (ΔG_r) obtained. When comparing the Rx, TS
16 and Pd points at the HS2ST: 4C_1 -IdoA, HS2ST: 2S_0 -IdoA, HS2ST: 1C_4 -IdoA, HS2ST: 1C_4 -GlcA, and
17 HS2ST: 4C_1 -GlcA complexes, we found that the network of non-covalent interactions engaged by
18 the active residues with the acceptor does not vary significantly (Figure S9-10). The reaction
19 proceeds by migration of the sulfate group from PAPS to the acceptor unit through an
20 asynchronous mechanism,⁴¹ where deprotonation of the nucleophile by H142 occurs at a later stage
21 in respect to the nucleophilic attack, while K83 stabilizes the migration of SO_3^- by protonating the
22 phosphate group on PAPS. While all the active site residues (K83, S86 and R80) display common
23 activity in all the investigated profiles, we found that only in HS2ST: 1C_4 -IdoA R288 protonates
24 the acceptor unit, anchoring the 1C_4 -IdoA in the active site. While the active site interaction
25 network remains unaltered, the activation barriers (ΔG^\ddagger) and reaction energies (ΔG_r) are strongly
26 affected by the puckering of the uronic acid. QM/MM calculations showed that the sulfation of
27 1C_4 , 2S_0 - and 4C_1 -IdoA are kinetically allowed paths ($\Delta G^\ddagger=15.4$, 18.4 and 9.3 kcal/mol
28 respectively), but only the sulfation of the most probable conformation 1C_4 is exoergonic.
29 Regarding GlcA, the computed ΔG^\ddagger s suggests that HS2ST prefers to catalyse the sulfation of 4C_1 -
30 GlcA (15.5 kcal/mol) over 1C_4 -GlcA (27.9 kcal/mol). HS2ST only recognizes and sulfates those
31 sugar conformers that are naturally occurring, and, therefore, physiologically relevant (1C_4 -IdoA,
32 and 4C_1 -GlcA). The sulfation of improbable puckers (1C_4 -GlcA) faces a barrier that is
33 unsurmountable under physiological conditions. To attain closer insights into HS2ST catalysis, a
34 detailed description of the catalytic mechanism and the role of active site residues is reported in
35 Discussion S2.
36
37
38
39
40
41
42
43
44
45
46
47
48
49
50
51
52
53
54
55
56
57
58
59
60

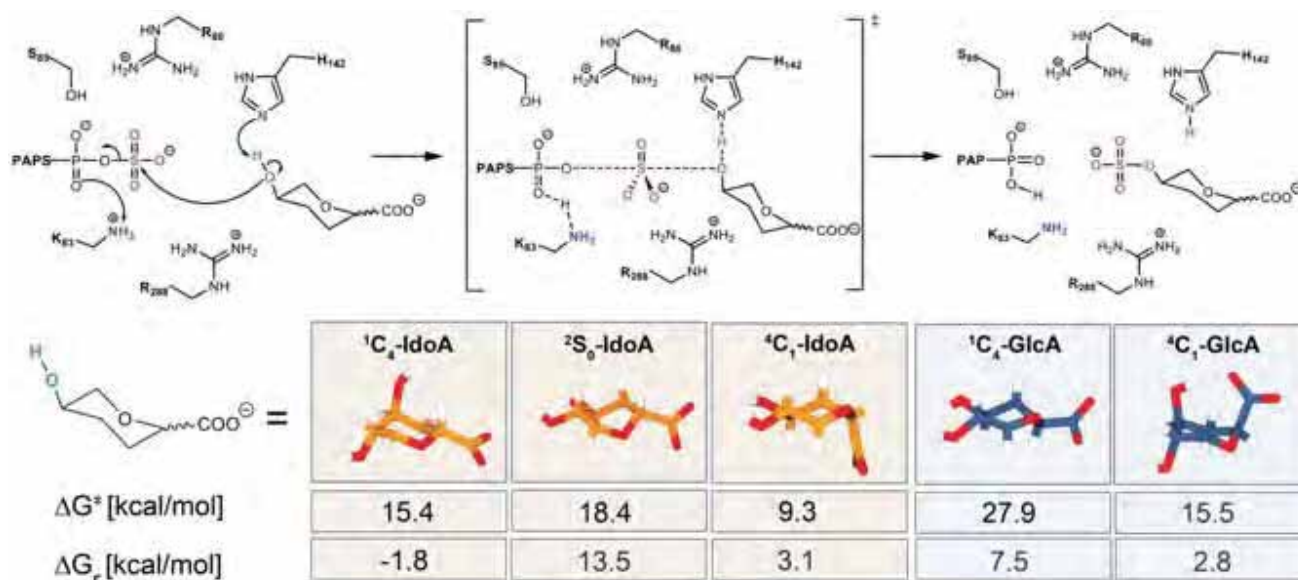
1
2
3
4
5
6
7
8
9
10
11
12
13
14
15
16
17
18
19
20
21
22
23
24
25
26
27
28
29
30
31
32
33
34
35
36
37
38
39
40
41
42
43
44
45
46
47
48
49
50
51
52
53
54
55
56
57
58
59
60

Figure 4. A schematic representation of the critical points computed at the ONIOM[M06-2X/6-31+G*:ff14SB] level of theory for HS2ST catalysis on ⁴C₁-, ²S₀- and ¹C₄-IdoA and ⁴C₁- and ¹C₄-GlcA saccharide units. The activation (ΔG^\ddagger) and reaction (ΔG_r) Gibbs free energies are reported.

HS6ST structural motions with different substrates.

In HS/heparin biosynthesis, 2-O-sulfation by HS2ST is followed by 6-O-sulfation by HS6ST. To explore the binding and catalytic processes exerted by HS6ST, we carried out molecular dynamics simulations using the catalytic domain of HS6ST bound to two different substrates (PDB ID 5T03 and 5T05).³² The PDB file 5T03 contains the HS6ST enzyme bound to a polysaccharide composed of **GlcNS**₊₁-GlcA₊₂-GlcNS₊₃-GlcA₊₄-GlcNS₊₅-GlcA₊₆, where **GlcNS**₊₁ is the acceptor sugar unit and GlcA₊₄ is the sugar unit that is specifically bound by a K131/K132 lysine clamp. This complex is hereafter referred to as HS6ST:GlcA₊₄. The PDB file 5T05 contains a HS6ST enzyme bound to a polysaccharide that varies from 5T03 only at position +4. 5T05, instead, contains a 2-O-sulfated IdoA2S in a ²S₀ skew boat conformation: **GlcNS**₊₁-GlcA₊₂-GlcNS₊₃-IdoA2S₊₄-GlcNS₊₅-GlcA₊₆,³² hereafter referred to as HS6ST:IdoA2S₊₄. The saccharide unit that undergoes sulfation is in position “+1” and indicated in bold.

The HS6ST active site contains two tryptophan residues,³² W153 and W210, that are solvent accessible (orange and yellow sticks in Figure 1C, respectively). The crystal structure 5T05 of HS6ST containing a 2-O-sulfate at position +4 (IdoA2S₊₄), shows the acceptor N-sulfo moiety GlcNS₊₁ within hydrogen bonding distance to the amide backbone of W210. The sidechain of

1
2
3
4
5
6
7
8
9
10
11
12
13
14
15
16
17
18
19
20
21
22
23
24
25
26
27
28
29
30
31
32
33
34
35
36
37
38
39
40
41
42
43
44
45
46
47
48
49
50
51
52
53
54
55
56
57
58
59
60

W210 points toward the GlcNS₊₁ acceptor in an unusual perpendicular orientation, that may allow CH- π interactions, *i.e.* typical aromatic-sugar interactions found in many glycan binding proteins.^{42, 43} In order to probe the presence of CH- π contacts between W210 and the acceptor glucosamine GlcNS₊₁ of both HS6ST:GlcA₊₄ and HS6ST:Ido2S₊₄, we analyzed the distance between the GlcNS₊₁ to the center of the indole phenyl ($d_{\text{CH}-\pi}$) and the angle between the CH vector and the phenyl ring plane normal vector ($\omega_{\text{CH}-\pi}$).⁴³⁻⁴⁵ Aside from the differences between HS6ST:GlcA₊₄ and HS6ST:IdoA2S₊₄, our analysis (see Discussion S3) does not meet the criteria for a classical or “T-shaped” CH- π interaction. Instead, W210 and the acceptor glucosamine interact via H-bonds in the HS6ST:Ido2S₊₄ complex (Figure S11A and B). This is confirmed by the MM-GBSA pairwise decomposition analysis: the binding affinity of W210 to the acceptor glucosamine GlcNS₊₁ (-11.4 ± 1.5 kcal/mol) is mainly due to electrostatics (-7.3 ± 2.0 kcal/mol), rather than to VDW interactions (-3.1 ± 0.9 kcal/mol) (Figure S12). QM calculations also confirm this behavior (Discussion S3), indicating that H-bonds, and non-hydrophobic interactions, are dominant in the GlcNS₊₁-W210 interaction. Worthy of note, the published structure of the N-sulfotransferase domain of the N-deacetylase/N--sulfotransferase (PDB ID 1NST)⁴⁶ contains a structurally conserved residue with the same topology as W210 (W713), an indication that this tryptophan in heparan sulfate N-deacetylase/N-sulfotransferases might play a similar role in binding GlcNAc. The positioning of W210 also resembles that of other solvent exposed tryptophan residues found in oligosaccharide lyases, such as W49 of *B. fragilis*-Beta-Lactamase⁴⁷ or W31 of *R. solanacearum* lectins.⁴⁸ As for these enzymes, the presence of W210 allows HS6ST to recognize a greater variety of ligands, conferring a degree of promiscuity to HS6STs.

The loop containing the other tryptophan residue W153 moves away from the active site, opening the active site cleft. We visualized this movement by plotting the distance between H158, the catalytic histidine, and the W153 indole sidechain center of mass for the HS6ST_{apo}, HS6ST:GlcA₊₄ and HS6ST:Ido2S₊₄ simulations in Figure 5A. For the apo enzyme, the distance between the center of mass for H158 and W153 fluctuates with an average amplitude of 5.3 Å, for HS6ST:GlcA₊₄, the distance between H158 and W153 varies substantially, with an amplitude of 4.4 Å while for HS6ST:IdoA2S₊₄ the distance is stable around 4.1 Å (Figure 5A).

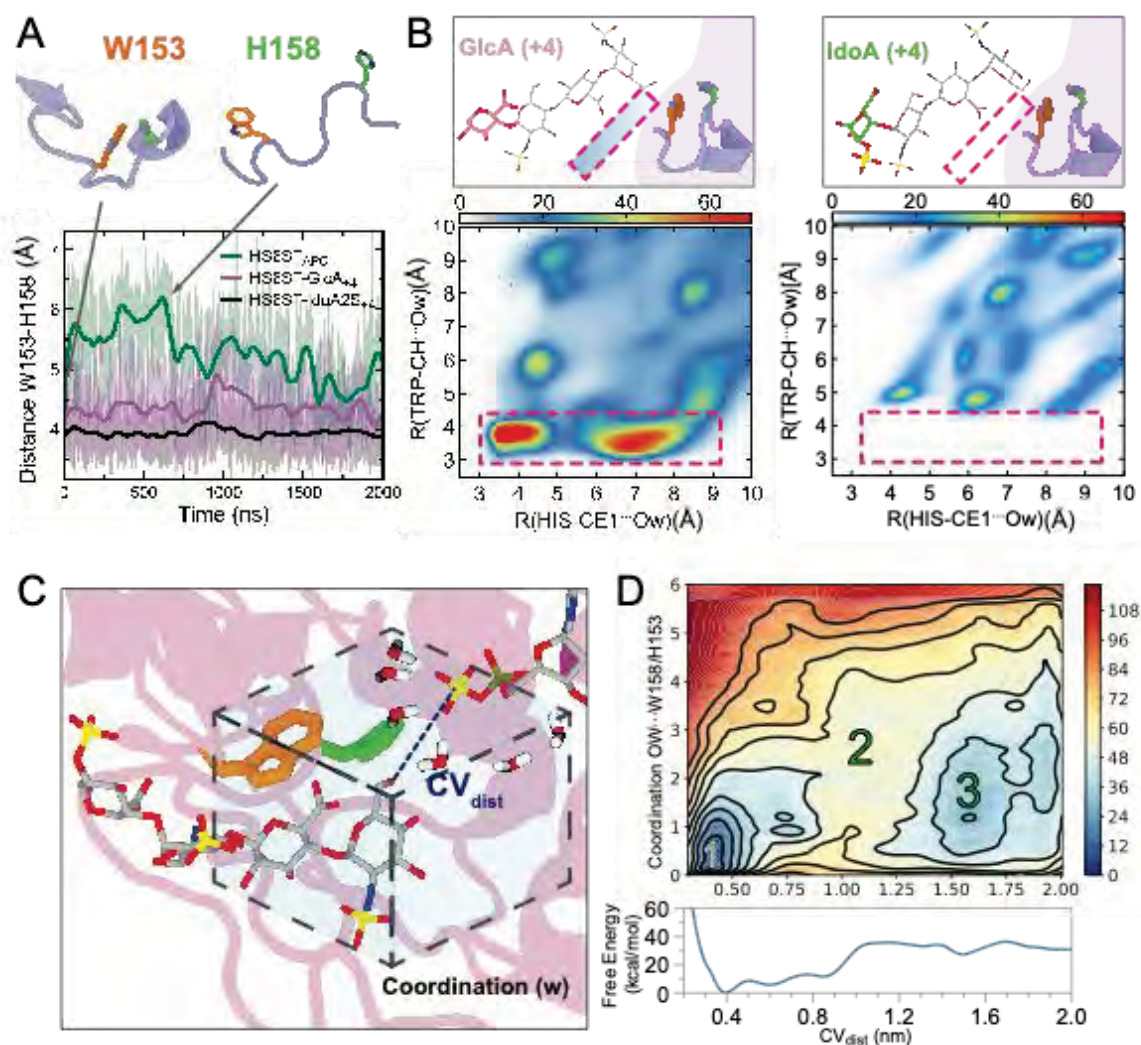


Figure 5. HS6ST substrate at position +4 influences HS6ST motility and active site hydration. **(A)** Distances between W153 and H158 during HS6ST simulations. **(B)** 2D-RDF function for the two closest atoms from W153 and H158 for both HS6ST:IdoA2S₊₄ and HS6ST:GlcA₊₄ simulations. Pink dashed lines outline the two water clusters observed in HS6ST:GlcA₊₄ simulations. Atoms are labeled according to AMBER force field nomenclature. **(C)** Diagrams of coordination parameters defined for free-energy calculations of active site hydration and acceptor coupling. The dashed box displays the coordination of waters surrounding the active site collective variable parameter (w). The substrate is shown as gray sticks. **(D)** Projection of the FES onto CV_{dist} and CV_w , as well as onto CV_{dist} alone (bottom). Numbers indicate the most relevant metastable states 1 and 3, separated by a high energy barrier, 2. Contours drawn every 12 kcal/mol.

1
2
3
4
5
6
7
8
9
10
11
12
13
14
15
16
17
18
19
20
21
22
23
24
25
26
27
28
29
30
31
32
33
34
35
36
37
38
39
40
41
42
43
44
45
46
47
48
49
50
51
52
53
54
55
56
57
58
59
60

Upon further analysis of the crystal structures, we observed that, while PDB ID 5T03 (HS6ST:GlcA₊₄) contained 4 structural water molecules at <4 Å from the catalytic histidine, PDB ID 5T05 (HS6ST:Ido2S₊₄) only had one. Based on the fact that PAPS is highly prone to hydrolysis and that HS6ST presents a shallow cleft architecture in its active site, we suggest that the presence of W153 could create a hydrophobic environment that protects PAPS^{49, 50} within the protein active site from oxidative damage.⁵¹ This prompted us to probe the effect of water on substrate binding to the active site of HS6ST:GlcA₊₄ and HS6ST:IdoA2S₊₄ complexes, by computing the radial distribution functions (RDF) of water molecules around H158. The weaker binding noted for HS6ST:GlcA₊₄ was found to affect solvent accessibility around the catalytic histidine, as shown by the radial distribution of water molecules 0.5g(r) for HS6ST:IdoA2S₊₄ and 1.0g(r) for HS6ST:GlcA₊₄ (Figure S13). Both HS6ST:GlcA₊₄ and HS6ST:IdoA2S₊₄ simulations display a typical hydrophilic interaction with a well-defined first hydration shell, showing a density peak at 2.0 Å and a second hydration shell around 3.8 Å (Figure S13A). As the simulations progressed for HS6ST:GlcA₊₄, interfacing residues became exposed to the solvent, facilitating glycan-water interaction and causing release of the substrate, and, with this, drifting of the substrate was observed. The persistence of structured water molecules between the enzyme and substrate during MD simulations was analyzed through normalized two-dimensional RDF functions (2D-RDF) for HS6ST:IdoA2S₊₄ and HS6ST:GlcA₊₄. Essentially, 2D-RDF calculates the pairwise value (Å distance) that reveals the hydrophobicity radius around the selected atom (Figure 5B). No water density was found at a distance below a radius of 4.8 Å from H158_{CE1} and W153_{CH} (Figure 5B, left and right panels), suggesting the absence of water molecules within the active site of HS6ST:IdoA2S₊₄. In contrast, for HS6ST:GlcA₊₄, the calculated pairwise value of water density was ~3.6 Å, showing two persistent water pockets for HS6ST:GlcA₊₄ at its binding interface (indicated with a pink rectangle in the left panel in Figure 5B). For HS6ST:GlcA₊₄, the average residence time for bridging water molecules within the active site was 277 ps, with the most persistent bridging molecule having a residence time of 737 ps, indicating that these water molecules are dynamically exchanged. During HS6ST:IdoA2S₊₄ simulations, W153 prevents the access of bulk water within a 4.3 Å radius of catalytic H158, while, in stark contrast, during HS6ST:GlcA₊₄ simulations, bulk water is able to permeate within 3.6 Å of H158. From the 2D-RDF analysis, we can conclude that W153 repulses water molecules more efficiently when +4 IdoA2S is the substrate (Figure 5B, left and right panels). In order to further explore how water

1
2
3 permeation around H158 and W153 precisely affects substrate binding, we calculated the free
4 energy of water coordination of HS6ST:IdoA2S₊₄ using well-tempered bias-exchange
5 metadynamics⁵² followed by corresponding reweighting techniques (Figure S14A).⁵³ The second
6 collective variable was defined as the region within H158 and W153 and their coordinating water
7 sites (w , Figure 5C). After calculating total residence times during the HS6ST:IdoA2S₊₄
8 simulations, the water shell shared by both residues averaged six water molecules, which was then
9 defined as the cutoff neighbor list.

10
11 The approximate free energy surface (FES) of substrate binding estimated as a function of
12 hydration was obtained by averaging the various unbinding runs. Figure 5C, right panel, shows
13 the free energy landscapes of water coordination at the active site as a function of substrate binding
14 state. Based on the conformational distributions at different water coordinations and CV_{dist} values,
15 the water shell around H158 is negatively correlated with stronger binding to the substrate (Figure
16 5C, right panel). Specifically, when there are three or more water molecules within W153/H158
17 ($w > 3$), the oligosaccharide substrate has one minimum at a bound configuration (distance of O6-S
18 ~ 4 Å, Figure 5C, right panel, basin 1). Interestingly, no minima exist for $w > 3$ when the
19 oligosaccharide substrate is in the unbound state (Figure 5C, right panel, basin 3). At high d values
20 (Figure 5C, right panel, basin 3, with the representative structure in Figure S14A, panel 3),
21 approximately two water molecules are coordinated to H158. As d decreases, water molecules are
22 expelled from the active site, showing that during binding, dehydration occurs in a stepwise
23 manner. This process of dehydration facilitates catalysis. The water molecules expelled from the
24 vicinity of H158 by W153 are replaced by native ligand contacts with the substrate (Figure 5C,
25 right panel, basin 1). All these features suggest that for HS6ST, the solvent plays a crucial role in
26 substrate recognition. Other subsites within HS6ST could influence its affinity for different
27 substrates and, consequently, its catalysis. In order to evaluate how overall enzyme motions affect
28 substrate affinity, we calculated the dynamic cross-correlation for HS6ST:IdoA2S₊₄ and
29 HS6ST:GlcA₊₄ simulations, and the results, reported in Supporting Material, suggest that the
30 K131/K132 loop works as a lid (Figure S15). This is in line with the current hypothesis that this
31 loop strongly binds to the negatively charged glycosaminoglycan chain and coordinates the
32 alignment of the glycan within the shallow active site.³² Based on the dynamic cross correlation
33 scores (see Discussion S4), the loops containing amino acids W210 and W153 are anti-correlated
34 in the apo structure (green squares, Figure S15, left panel), confirming that the tryptophan residues
35
36
37
38
39
40
41
42
43
44
45
46
47
48
49
50
51
52
53
54
55
56
57
58
59
60

(W153/W210) flanking the catalytic histidine in HS6STs play a role in promoting the binding of the acceptor. We investigated the impact of the K131/K132 loop for both HS6ST:GlcA₊₄ and HS6ST:IdoA2S₊₄ by calculating MM-GBSA values, finding that K131 binds with a weaker binding energy to the GlcA₊₄ acceptor when compared to IdoA2S₊₄, with values of -6.4 ± 1.1 kcal/mol and -11.8 ± 0.4 kcal/mol, respectively (Figure S12). Thus, these tryptophan residues, that are unique to HS6STs, could convey, at least in part, the substrate specificity (albeit with some promiscuity) of this enzyme.

HS6ST sulfotransferase hydration and molecular recognition.

HS6ST presents unique structural characteristics that differ substantially from the reported binding interfaces for HSNST,⁴⁶ HS2ST,³⁴ and HS3ST.^{14, 32} Compared to HS2ST, fewer contacts exist between HS6ST and its substrate;³² only the first four units of a polysaccharide substrate form contacts with HS6ST, versus all units of a heptasaccharide for HS2ST.³⁵ In order to understand the dynamics of the enzyme-substrate interactions in HS6ST:GlcA₊₄ and HS6ST:IdoA2S₊₄ complexes, we carried out interaction fingerprinting analysis. In this type of analysis, the interactions engaged by the residues with the monosaccharide units are classified into water bridge, salt bridge, and hydrogen-bond donor and acceptor. Contacts are expressed based on the frequency (%) with which they appear during the dynamics simulations. While interaction fingerprinting was performed for all oligosaccharide binding residues for both HS6ST:GlcA₊₄ and HS6ST:IdoA2S₊₄ conditions, we focused our analysis on W153/W210, which surrounds the acceptor, and the K131/K132 loop. While the HS6ST:IdoA2S₊₄ K131/K132 pair maintains H-bonds and salt bridges with IdoA2S₊₄ throughout most of the simulation time (>90%), these interactions are lost for GlcA₊₄ (~0.05%, Figure S17A-B, bottom panels). These interactions are shifted from GlcA₊₄ to GlcNS₊₁/GlcA₊₂, indicating that as the chain dissociates from its original binding position it is capable of binding at different locations. The nature of the K131/K132 interactions and contacts with GlcA₊₄ for the HS6ST:GlcA₊₄ simulations is not sufficient to keep the reducing end fully bound to the enzyme (Figure S17). GlcA₊₄ loses water bridges and hydrogen bonds with W153, T151 and Q130. This loss of interactions impacts water access to the HS6ST active site: the water shell around GlcNS₊₁ is 50% higher during HS6ST:GlcA₊₄ simulations when compared to HS6ST:IdoA2S₊₄. These data indicate tighter binding of K131/K132 with IdoA2S₊₄, when compared to GlcA₊₄, preventing water access at the protein acceptor interface. Dislodging a

polysaccharide involved in an extensive network of water mediated hydrogen bonds poses a major challenge for HS6ST. The loss of contacts between the enzyme and substrate observed during the HS6ST:GlcA₊₄ simulations not only impact the enzyme at the reducing end, as previously discussed, but also at the NRE (see Figure S17 and Discussion S5).

Sulfate transfer to the 6O-position.

To obtain further information on how HS6ST catalyzes the SO₃⁻ transfer to the ligand, we investigated the reaction mechanism of GlcNS sulfation for the HS6ST:GlcA₊₄ complex. We found that the reaction proceeds via a S_N2-like asynchronous mechanism (as shown in Figure 6), and that the sulfation requires 16.1 kcal/mol, in line with the results obtained for HS2ST, suggesting that the activation energy is easily surmountable under physiological conditions. To demonstrate a catalytic role for K104 and H158,³⁵ we manually mutated the sidechain of K104, replacing the -CH₂NH₃⁺ terminal group for a CH₃, and mutated the H158 as H158A, in order to abolish their potential effects within the active site of HS6ST:GlcA₊₄. In line with the experimental mutagenesis results obtained by Xu and colleagues,³² we found that elimination of the terminal NH₃⁺ group in K104 raises the activation energy up to 48.2 kcal/mol, while H158A raises it to 24.9 kcal/mol, confirming that K104 and H158 are crucial for HS6ST catalysis. A detailed representation and description of the critical points obtained for HS6ST catalysis are given in Figure S19 and Discussion S6, respectively.



Figure 6. A schematic representation of the critical points computed at the ONIOM[M06-2x/6-31+G*:ff14SB] level of theory for HS6ST catalysis.

HS6ST at the non-reducing end of the glycan.

Natural substrate for HS6STs are sugar oligomers that are much longer than the polysaccharide that was co-crystallized with HS6ST. Hence, we systematically evaluated an expansion of the

1
2
3 HS6ST ideal substrate, IdoA2S₊₄, with a polysaccharide to further explore binding at the NRE of
4 HS6ST. The final models were composed of the HS6ST enzyme (PDB ID 5T05) containing its
5 crystal bound substrate plus a polysaccharide extension with varying degrees of modifications:
6
7
8 (GlcNX-GlcAX/IdoAX)_{x4}-GlcNS₊₁-GlcA₊₂-GlcNS₊₃-IdoA2S₊₄-GlcNS₊₅-GlcA₊₆. These
9 additions consisted of (I) GlcNS6S-IdoA2S, (II) GlcNS-IdoA, (III) GlcNS-GlcA2S and (IV)
10 GlcNAc-GlcA. All models were subjected to molecular dynamics simulations for 1 μs and each
11 enzyme-monosaccharide interaction was fingerprinted. For extension I, GlcNS6S-IdoA2S, the
12 least probable substrate for HS6ST, was placed at the NRE.
13
14
15
16

17 In this case, the substrate (IdoA2S_{.3} and IdoA2S_{.5}) formed water/salt bridges and hydrogen bonds
18 with both R112 and R329 (Figure S19). R116 bound to both GlcNS_{.4} and Ido2S_{.5}, and Ido2S_{.5}
19 bound to R112 and R329 with a higher frequency than R116. Closer to the acceptor GlcNS, GlcA_{.1}
20 formed most contacts with R112/R148/R206 and K104. This network of positively charged
21 residues surrounding GlcA_{.1} was persistent across all models assayed, but the nature of interactions
22 shifted from mainly hydrogen bonds and salt bridges to water bridges for the less sulfated
23 substrates. For extensions II and III, which were GlcNS-IdoA and GlcNS-GlcA2S, respectively,
24 contacts at positions -4 to -6 were composed of water bridges, with a notable new hydrogen bond
25 being formed between the GlcNS_{.2} and H203. Interestingly, the binding profiles of substrates II
26 and III were similar, despite the absence of 2-O-sulfation on substrate II. This emphasizes the
27 importance of epimerization of the uronic acid for increasing chain flexibility, improving glycan
28 binding. K202, R206 and R329 form hydrogen bonds and water bridges with IdoA/GlcA2S_{.3},
29 indicating their probable importance as selectors of sulfated uronic acid at this position.
30 Reinforcing this idea, K202 and R206 did not bind the -3 substrate when GlcNS_{.2} was 6-O-
31 sulfated. H203, suggested to have a role in binding the -2-moiety and orienting the acceptor for
32 catalysis,³² formed hydrogen bonds with the GlcNS of substrates II and III, while forming
33 hydrophobic interactions with substrate IV, which only contains GlcNAc-GlcA. This suggests that
34 H203 plays a critical role not as an active site residue but as an extended binding residue orienting
35 the acceptor when the glucosamine is not 6-O-sulfated and binding to the -2 glucosamine in either
36 acetylated or sulfated forms. Tornberg and colleagues previously reported that the mutation R323Q
37 in the HS6ST isoform 1 (*HS6ST1*) gene is correlated with idiopathic hypogonadotropic
38 hypogonadism (IHH) in humans.⁵⁴ The corresponding HS6ST residue in zebrafish is R329.^{32, 54}
39
40
41
42
43
44
45
46
47
48
49
50
51
52
53
54
55
56
57
58
59
60

1
2
3 when the substrate had a GlcNS or GlcNAc at -2 (Figure S19, panels (-2)). However, when the
4 substrate at -2 was a GlcNS6S, R329 formed fewer (<20% of the dynamics course) hydrogen
5 bonds as an acceptor of $-C_6SO_3^-$, suggesting that this residue plays a role as a processivity gate
6 towards the NRE of the polysaccharide. Beyond its role as a selector for NRE sulfation, R329
7 appears to play a role in allosterically regulating PAPS access to the active site. When analyzing
8 the HS6ST_{apo} simulations we identified that the loop containing R329 is highly mobile and, in the
9 absence of a substrate, R329 formed a salt bridge with D192 (Supporting Video 1). This loop
10 closure occludes the PAPS binding site and reduces the pocket volume from 181 (open loop) to 6
11 cubic Å³, as calculated by POVME 3.0.⁵⁵ Thus, this salt bridge could function as the homotropic
12 regulator controlling PAPS binding site access since, upon substrate binding, the R329/D192
13 bridge would be dissolved. This idea is strengthened after calculating the pairwise interaction
14 energies using MM-GBSA between the R329-D192 pair during the apo simulations (-12.3±0.2
15 kcal/mol) with R329 and GlcS₊₃/Idoa2S₊₄/GlcNS₊₅ (-4.9±0.1, 15.7±0.6, 1.9±0.3 kcal/mol) (Figure
16 7A). We hypothesized that the topology of R329/D192 residues influences PAPS binding, and,
17 consequently, glycan secondary modifications. To confirm this hypothesis experimentally, we
18 conducted systematic *in vitro* site-directed mutagenesis of HS6ST R329 and D192. Mutants
19 carrying a single conservative replacement, D192E and R329K, were designed, as was a double
20 mutant, D192E/R329K. Alanine substitutive mutants were also synthesized and expressed. Wild-
21 type enzymes and mutants were incubated with a hexasaccharide substrate composed of repeating
22 GlcNS-IdoA2S units and the sulfate donor PAPS, and, thereafter, the product analyzed using SAX-
23 HPLC chromatography, as described in the Methods Section. Two mutations show reduced
24 activity; specifically, D192E showed a 50% reduction in activity and R329K showed a 43%
25 reduction in activity when compared to the wild-type enzyme. Substituting the conserved residues
26 R329 and D192 to an alanine leads to a 95% reduction of 6-O-sulfation (Figure 7B). This finding
27 suggests that after substrate binding, R329 interacts with units -1/-2, breaking its saline bridge with
28 D192, possibly acting as a homotropic allosteric modulator of PAPS binding. Strikingly, when we
29 compared the sequence of HS6STs to the sequence of all Golgi sulfotransferases verified in the
30 NCBI and UniProt databases, we found that these residues are conserved within the whole
31 glycosaminoglycan sulfotransferase family (Figure 7C). This suggests that the mechanism by
32 which this salt bridge is outcompeted by substrate binding allowing PAPS access is conserved
33 among this family of proteins.
34
35
36
37
38
39
40
41
42
43
44
45
46
47
48
49
50
51
52
53
54
55
56
57
58
59
60

1
2
3 **HS2ST and HS6ST share key molecular features but differ drastically in their substrate**
4 **recognition.**
5

6
7 While our data suggest many similarities in the catalytic mechanism of HS2ST and HS6ST, we
8 found that substrate binding modes varied considerably. Since the sulfate transfer requires a
9 hydrophobic environment to protect PAPS from hydrolysis, we calculated the electrostatic surface
10 potentials of both HS2ST and HS6ST using Adaptive Poisson–Boltzmann Solver (APBS).⁵⁶ As
11 shown in Figure S21A and B, both enzymes present an extended patch of positive amino acids
12 within their binding cleft. Because the positively charged patch (blue regions) is spatially close to
13 the hydrophobic active site (white patches), we investigated the interplay between these two
14 regions with antagonistic characteristics. We could observe that both sulfotransferase enzymes
15 present a large, discrete patch of positively charge residues, indicating that the macromolecular
16 interface of these enzymes is dominated by electrostatic interactions. This topology is similar to
17 protein–DNA binding systems, where one-dimensional diffusion (sliding) is promoted mainly by
18 electrostatic forces, while specific interactions involving hydrogen bonds and van der Waals forces
19 are absent.^{57,58}
20
21
22
23
24
25
26
27
28

29 Water molecules that are strongly bound at the ligand binding region of the enzyme can have a
30 crucial effect on the overall ligand binding energy, since they must be displaced to allow the ligand
31 to access the binding site.^{57, 59, 60} We computed the displacement of perturbed water upon binding
32 by the grid based on the homogeneous inhomogeneous solvation theory (GIST) for HS2ST_{apo} and
33 HS6ST_{apo} enzymes.⁶⁰ The resulting calculated free energy of solvation for each residue within the
34 binding cleft provides quantitative data on hydrophobicity and solvent accessibility, and the
35 solvation free energy grid is mapped onto the protein surfaces in Figure 7D. Hydrophobicity is a
36 metric to calculate the solvation free energy that would need to be replaced by a ligand binding
37 into the enzyme substrate binding region. Green patches show residues that require more energy
38 to be desolvated (higher negative solvation free energy), while water molecules can be more easily
39 displaced from purple regions. A comparison of localized hydrophobicity within both
40 sulfotransferase binding interfaces demonstrates the hydrophobic nature of the PAPS binding site.
41 HS2ST S85 and HS6ST T108, known to bind and orient PAPS towards catalysis, are the interface
42 binding site residues displaying higher hydrophobicity. HS2ST ARG/LYS clamps show a similar
43 solvation energy (~-6.0 kcal/mol) and T87, a conserved residue amongst all sulfotransferases, is
44 critical for maintaining the PAPS phosphate equatorially positioned showing the highest
45
46
47
48
49
50
51
52
53
54
55
56
57
58
59
60

hydrophobicity within the protein interface (~ -0.6 kcal/mol). HS6ST W210, and the loop K131/K132 display the highest solvent exposure (~ -12.0 kcal/mol), while W153 maintains a hydrophobic environment around the catalytic H158.

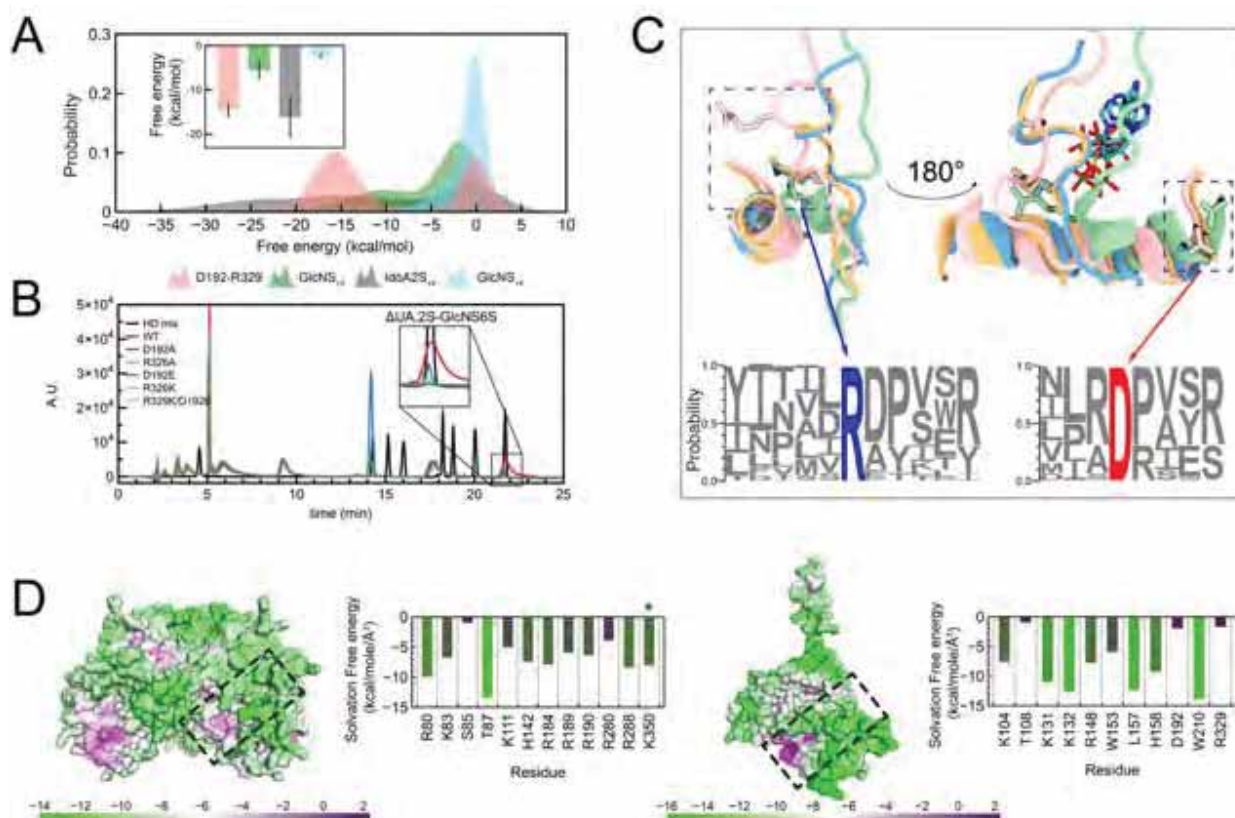


Figure 7. A primer on shared topologies of heparin sulfotransferases. **(A)** Probability distribution of calculated pairwise energies during molecular dynamics simulations for (I) the substrate IdoA2S-GlcNS and (II) the D192-R329 salt bridge during HS6ST apoprotein simulations. The insert shows calculated averages. **(B)** SAX-HPLC analysis of total disaccharide composition after the action of R329/D192 mutants incubated with IdoA2S-GlcNS substrates. The insert highlights the formation of IdoA2S-GlcNS6S moieties. HD mix (black line), heparin disaccharide mix (Iduron, UK). **(C)** A salt bridge is conserved amongst glycan sulfotransferases and its conformation change is triggered by substrate binding. Superposition of HSSTs: light blue, HSNST; pink, HS2ST; orange, HS3ST and green HS6ST. Bottom logo plot highlights ARG (blue) and ASP (red) conservation amongst all HSSTs known to date. **(D)** Calculated solvation free energies on the surface of the binding interfaces of HS2ST (left) and HS6ST (right) as a measure of their hydrophobicity. Tables show per-residue average hydrophobicity for each apoprotein

1
2
3 enzyme. Table colors range from more hydrophobic (purple), to more hydrophilic (green). The
4 asterisk denotes C-terminal “prime” residues.
5
6
7

8
9 We speculated that the strong H-bonding of W210 to the glucosamine acceptor reduces the
10 ability of HS6STs to discriminate among oligosaccharides based on their specific sulfation and
11 epimerization patterns. To counteract this, the K131/K132 loop acts as a “preference” selector.
12 This role is emphasized when we look at the anatomy of the floppy K131/K132 loop, that is N-
13 and C-terminally flanked by two prolines - P123 and P139 - which are conserved among all
14 HS6STs. The presence of prolines flanking protein loops has been shown to drastically limit loop
15 conformations^{61, 62} and to reduce loop elasticity,^{63, 64} a phenomenon termed “focused motional
16 freedom”. These studies have shown that rigidity is introduced by the proline pyrrolidine ring,
17 drastically limiting the backbone dihedral angle to 90°. As the polysaccharides are gradually
18 sulfated during the biosynthetic process, negative charges build up and polymer hydrophilicity
19 increases. Intuitively, this should also increase the binding entropy of substrates to the positively
20 charged binding sites. Because HS6ST acts relatively late within HS biosynthesis, this
21 accumulating negative charge causes a difficult task for the enzyme - HS6ST needs to recognize
22 its substrates with a reasonable degree of flexibility and promiscuity without irreversibly binding
23 them. The events leading to sulfate transfer are remarkably different for HS2ST. We can assume
24 that to achieve processivity the enzyme should bind moderately to its polymer substrate. Upon
25 binding of the substrate, the swapped C-terminal tail of the HS2ST adjacent monomer bends over
26 and orients the substrate - this compound enzyme interface allows it to completely burry the
27 oligosaccharide, increasing its interaction surface to maintain the large oligosaccharide in a semi-
28 enclosed position, facilitating its processivity. The difference between APO conformations and
29 substrate-bound HS2STs poses indicates the formation of specific and extensive interactions
30 between HS2ST and its cognate substrates, enabling specific discrimination between anomeric or
31 epimeric moieties and size. The influence of motion in cleft/active site recognition has also been
32 described for other glycan binding proteins.⁶⁵⁻⁶⁷
33
34
35
36
37
38
39
40
41
42
43
44
45
46
47
48
49
50

51 **Conclusion**

52
53
54
55
56
57
58
59
60

1
2
3 Here we analyzed the substrate-binding modes and catalysis of the HS biosynthetic
4 sulfotransferases HS2ST and HS6ST. Our QM/MM results highlight common features between
5 the two enzymes - they promote the sulfate transfer from PAPS to the respective acceptor unit in
6 a S_N2 -like mechanism with a histidine as the catalytic base and a lysine stabilizing the formation
7 of 5'-phosphate group on PAPS. Our molecular dynamics simulations, however, revealed
8 important differences between HS2ST and HS6ST during substrate recognition, evidencing the
9 molecular determinants required for each enzyme to selectively recognize and distinguish among
10 a pool of substrates.
11
12

13
14
15
16
17 For HS2ST, we investigated the affinity of this enzyme toward IdoA or GlcA, starting from the
18 available crystal structure which presents IdoA in the 4C_1 conformation; then, we analyzed the
19 effect of different uronic acid puckers within the substrate. Overall, we identified, by *in silico*
20 methods, three structural determinants for substrate specificity: an electrostatic fork made of
21 R184/R189 and R288, two molecular clamps (K111/R190 and R288/K350') and R80, which
22 anchors the glucosamine at position +2. The group of three arginines forms a positively charged
23 fork that anchors the ligand by entrapping the C_6 carboxyl group of the uronic acid acceptor unit.
24 This arginine fork is able to recognize GlcA or IdoA epimers and their puckers but prefers the
25 carboxyl group of 1C_4 -IdoA that fits properly within the electrostatic trap. The two molecular
26 clamps identified (K111/R190 and R288/K350') position the ligand precisely within the active
27 site, while R80 is responsible for recognizing the GlcN2S unit at +2 position, reinforcing the
28 hypothesis that N-sulfation is a prerequisite for 2-O-sulfation.³⁴
29
30
31
32
33
34
35
36
37
38

39 The role of R189 in steric hindrance of GlcA was further investigated by *in vitro* enzymatic
40 assays, suggesting this residue is a vital component of the fork that determines the increased
41 preference of HS2ST for iduronate. By calculating binding affinities, we found that HS2ST
42 preferably recognizes IdoA over GlcA and, moreover, the enzyme senses the conformation of the
43 sugar ring, binding to the most energetically favorable conformations (${}^1C_4/{}^2S_0$ of IdoA). The
44 preference of HS2ST for ligands with the most plausible sugar conformations was confirmed by
45 the energetic profiles computed for the catalytic mechanism, which suggest that even if the
46 conformation flexibility of the enzyme allows the binding of different epimers/puckers, HS2ST
47 preferably sulfates 1C_4 -IdoA over any other puckers and epimers. Overall, we provide evidence,
48 at an atomic level, explaining how HS2ST displays a preference for IdoA over GlcA residues as
49 acceptor units.
50
51
52
53
54
55
56
57
58
59
60

1
2
3 HS6ST binding cleft is unique when compared to HS2ST and other glycosaminoglycan
4 sulfotransferases. Our data identifies a set of unique structural determinants: W153, W210 and a
5 R329/D192 salt bridge. The narrow binding cleft presents two solvent exposed tryptophan residues
6 (W153 and W210) that flank the catalytic histidine at the active site. Our data indicate that W153,
7 with assistance of the K131/K132 loop, maintains active site hydrophobicity by repelling solvent
8 molecules from the catalytic center. Our observations suggest that water dynamics play an integral
9 role in HS6ST substrate binding and dissociation since the enzyme must compete with the bulk
10 solvent to bind to a highly sulfated/hydrated substrate which is extremely hydrophilic. W210 helps
11 bind the acceptor substrate by engaging a H-bond with the acceptor unit.

12
13 Furthermore, we identified a salt bridge formed between R329 and D192 that blocks the cofactor
14 entry of HS6ST. Upon substrate binding, this non-covalent bond breaks allowing access to the
15 PAPS donor. This bridge is conserved within the heparin/HS sulfotransferase family and, to the
16 best of our knowledge, has not previously been described. This novel structural signature can act
17 as a gate that opens allowing PAPS to access its binding site, working as a homotropic regulator.
18 This understanding has obvious implications on sulfotransferase design, opening questions for
19 future investigations on how PAPS accesses the binding cleft of these enzymes.
20
21
22
23
24
25
26
27
28
29
30
31

32 **Supporting Information**

33 The Supporting Information is available free of charge on the ACS Publications website.
34

35
36
37
38 Methods, detailed analysis of all enzyme complexes conditions investigated and supporting figures
39 and table (PDF).
40

41
42
43 Video S1. (MP4).
44

45
46
47 Cartesian coordinates for critical points (reactant, transition state and product) obtained at a
48 QM/MM level.
49

50
51
52 Corresponding author email:

53
54 *tgferrei@central.uh.edu
55
56
57
58
59
60

Funding Sources

This study was supported in part by funds from UH SeFAC (VJCT), Mizutani Foundation (VJCT), R01 EY029289 (VJCT), European Union (Marie Skłodowska Curie Actions SUPA-HD 625451) (JWM).

ACKNOWLEDGMENT

The authors acknowledge the use of the Opuntia Cluster and the advanced support from the Center of Advanced Computing and Data Science at the University of Houston and the Texas Advanced Computing Center (TACC) at The University of Texas at Austin for providing High Performance Computing resources. URL: <http://www.tacc.utexas.edu>. The authors would like to thank Francisco Corzana and Søren Balling Engelsen for providing the 2D-RDF source code and Michael Williams for helping with code development. Carbohydrate analysis was supported by the U.S. Department of Energy, Office of Science, Basic Energy Sciences, Chemical Sciences, Geosciences and Biosciences Division, under award #DE-SC001566 to Paarstoo Azadi.

ABBREVIATIONS

IdoA, α -L-Iduronic acid; GlcA, β -D-Glucopyranuronic acid; HS2ST, Heparan sulfate 2-O-sulfotransferase; HS6ST, Heparan sulfate 2-O-sulfotransferase; PAPS, 3'-phosphoadenosine-5'-phosphosulfate; HPLC, High Performance Liquid Chromatography; NRE, non-reducing end.

REFERENCES

1. Nader, H. B.; Dietrich, C. P.; Buonassisi, V.; Colburn, P., Heparin sequences in the heparan sulfate chains of an endothelial cell proteoglycan. *Proc Natl Acad Sci U S A* **1987**, *84* (11), 3565-9.
2. Gesteira, T. F.; Coulson-Thomas, V. J.; Ogata, F. T.; Farias, E. H.; Cavalheiro, R. P.; de Lima, M. A.; Cunha, G. L.; Nakayasu, E. S.; Almeida, I. C.; Toma, L.; Nader, H. B., A novel approach for the characterisation of proteoglycans and biosynthetic enzymes in a snail model. *Biochim Biophys Acta* **2011**, *1814* (12), 1862-9.
3. Attreed, M.; Saied-Santiago, K.; Bulow, H. E., Conservation of anatomically restricted glycosaminoglycan structures in divergent nematode species. *Glycobiology* **2016**, *26* (8), 862-870.
4. *Heparin Market Size, Share & Trends Analysis Report By Type (Low Molecular Weight, Ultra-low Molecule Weight)*. Grand View Research. <https://www.grandviewresearch.com/industry-analysis/heparin-market>, Accessed December 15, 2019.
5. Gallagher, J. T.; Walker, A., Molecular distinctions between heparan sulphate and heparin. Analysis of sulphation patterns indicates that heparan sulphate and heparin are separate families of N-sulphated polysaccharides. *Biochem J* **1985**, *230* (3), 665-74.
6. Shriver, Z.; Capila, I.; Venkataraman, G.; Sasisekharan, R., Heparin and heparan sulfate: analyzing structure and microheterogeneity. *Handb Exp Pharmacol* **2012**, (207), 159-76.

- 1
2
3
4 7. Hileman, R. E.; Fromm, J. R.; Weiler, J. M.; Linhardt, R. J., Glycosaminoglycan-protein
5
6 interactions: definition of consensus sites in glycosaminoglycan binding proteins. *Bioessays*
7
8 **1998**, *20*(2), 156-67.
- 9
10
11 8. Tykesson, E.; Mao, Y.; Maccarana, M.; Pu, Y.; Gao, J.; Lin, C.; Zaia, J.; Westergren-
12
13 Thorsson, G.; Ellervik, U.; Malmstrom, L.; Malmstrom, A., Deciphering the Mode of Action of
14
15 the Processive Polysaccharide Modifying Enzyme Dermatan Sulfate Epimerase 1 by Hydrogen-
16
17 Deuterium Exchange Mass Spectrometry. *Chem Sci* **2016**, *7*(2), 1447-1456.
- 18
19
20
21 9. Mandon, E.; Kempner, E. S.; Ishihara, M.; Hirschberg, C. B., A monomeric protein in
22
23 the Golgi membrane catalyzes both N-deacetylation and N-sulfation of heparan sulfate. *J Biol*
24
25 *Chem* **1994**, *269*(16), 11729-33.
- 26
27
28
29 10. Li, J.; Hagner-McWhirter, A.; Kjellen, L.; Palgi, J.; Jalkanen, M.; Lindahl, U.,
30
31 Biosynthesis of heparin/heparan sulfate. cDNA cloning and expression of D-glucuronyl C5-
32
33 epimerase from bovine lung. *J Biol Chem* **1997**, *272*(44), 28158-63.
- 34
35
36
37 11. Sugahara, K.; Kitagawa, H., Recent advances in the study of the biosynthesis and
38
39 functions of sulfated glycosaminoglycans. *Curr Opin Struct Biol* **2000**, *10*(5), 518-27.
- 40
41
42 12. Nagai, N.; Habuchi, H.; Esko, J. D.; Kimata, K., Stem domains of heparan sulfate 6-O-
43
44 sulfotransferase are required for Golgi localization, oligomer formation and enzyme activity. *J*
45
46 *Cell Sci* **2004**, *117*(Pt 15), 3331-41.
- 47
48
49 13. Nader, H. B.; Dietrich, C. P., Effect of heparin sulfate fractions on coagulation and
50
51 hemostasis. *Proc Soc Exp Biol Med* **1974**, *146*(2), 504-8.
- 52
53
54
55
56
57
58
59
60

- 1
2
3
4 14. Moon, A. F.; Edavettal, S. C.; Krahn, J. M.; Munoz, E. M.; Negishi, M.; Linhardt, R.
5
6 J.; Liu, J.; Pedersen, L. C., Structural analysis of the sulfotransferase (3-o-sulfotransferase
7
8 isoform 3) involved in the biosynthesis of an entry receptor for herpes simplex virus 1. *J Biol*
9
10 *Chem* **2004**, *279*(43), 45185-93.
11
12
13
14 15. Nader, H. B.; Buonassisi, V.; Colburn, P.; Dietrich, C. P., Heparin stimulates the
15
16 synthesis and modifies the sulfation pattern of heparan sulfate proteoglycan from endothelial
17
18 cells. *J Cell Physiol* **1989**, *140*(2), 305-10.
19
20
21 16. Coulson-Thomas, V. J., The role of heparan sulphate in development: the ectodermal
22
23 story. *Int J Exp Pathol* **2016**, *97*(3), 213-29.
24
25
26 17. Coulson-Thomas, V. J.; Chang, S. H.; Yeh, L. K.; Coulson-Thomas, Y. M.;
27
28 Yamaguchi, Y.; Esko, J.; Liu, C. Y.; Kao, W., Loss of corneal epithelial heparan sulfate leads to
29
30 corneal degeneration and impaired wound healing. *Invest Ophthalmol Vis Sci* **2015**, *56*(5),
31
32 3004-14.
33
34
35 18. Coulson-Thomas, V. J.; Gesteira, T. F.; Esko, J.; Kao, W., Heparan sulfate regulates
36
37 hair follicle and sebaceous gland morphogenesis and homeostasis. *J Biol Chem* **2014**, *289*(36),
38
39 25211-26.
40
41
42 19. Guibinga, G. H.; Miyanochara, A.; Esko, J. D.; Friedmann, T., Cell surface heparan
43
44 sulfate is a receptor for attachment of envelope protein-free retrovirus-like particles and VSV-G
45
46 pseudotyped MLV-derived retrovirus vectors to target cells. *Mol Ther* **2002**, *5*(5 Pt 1), 538-46.
47
48
49 20. Thacker, B. E.; Seamen, E.; Lawrence, R.; Parker, M. W.; Xu, Y.; Liu, J.; Vander
50
51 Kooi, C. W.; Esko, J. D., Expanding the 3-O-Sulfate Proteome--Enhanced Binding of
52
53
54
55
56
57
58
59
60

1
2
3
4 Neuropilin-1 to 3-O-Sulfated Heparan Sulfate Modulates Its Activity. *ACS Chem Biol* **2016**, *11*
5
6 (4), 971-80.
7

8
9 21. Gunal, S.; Hardman, R.; Kopriva, S.; Mueller, J. W., Sulfation pathways from red to
10
11 green. *J Biol Chem* **2019**, *294* (33), 12293-12312.
12

13
14 22. Merry, C. L.; Bullock, S. L.; Swan, D. C.; Backen, A. C.; Lyon, M.; Beddington, R.
15
16 S.; Wilson, V. A.; Gallagher, J. T., The molecular phenotype of heparan sulfate in the Hs2st-/
17
18 mutant mouse. *J Biol Chem* **2001**, *276* (38), 35429-34.
19
20

21
22 23. Kamimura, K.; Koyama, T.; Habuchi, H.; Ueda, R.; Masu, M.; Kimata, K.; Nakato,
23
24 H., Specific and flexible roles of heparan sulfate modifications in Drosophila FGF signaling. *J*
25
26 *Cell Biol* **2006**, *174* (6), 773-8.
27

28
29 24. Esko, J. D.; Selleck, S. B., Order out of chaos: assembly of ligand binding sites in
30
31 heparan sulfate. *Annu Rev Biochem* **2002**, *71*, 435-71.
32

33
34 25. Bullock, S. L.; Fletcher, J. M.; Beddington, R. S.; Wilson, V. A., Renal agenesis in mice
35
36 homozygous for a gene trap mutation in the gene encoding heparan sulfate 2-sulfotransferase.
37
38 *Genes Dev* **1998**, *12* (12), 1894-906.
39
40

41
42 26. Wilson, V. A.; Gallagher, J. T.; Merry, C. L., Heparan sulfate 2-O-sulfotransferase
43
44 (Hs2st) and mouse development. *Glycoconj J* **2002**, *19* (4-5), 347-54.
45

46
47 27. Bethea, H. N.; Xu, D.; Liu, J.; Pedersen, L. C., Redirecting the substrate specificity of
48
49 heparan sulfate 2-O-sulfotransferase by structurally guided mutagenesis. *Proc Natl Acad Sci U S*
50
51 *A* **2008**, *105* (48), 18724-9.
52
53
54
55
56
57
58
59
60

- 1
2
3
4 28. Atha, D. H.; Stephens, A. W.; Rosenberg, R. D., Evaluation of critical groups required
5
6 for the binding of heparin to antithrombin. *Proc Natl Acad Sci U S A* **1984**, *81* (4), 1030-4.
7
8
9 29. Habuchi, H.; Tanaka, M.; Habuchi, O.; Yoshida, K.; Suzuki, H.; Ban, K.; Kimata, K.,
10
11 The occurrence of three isoforms of heparan sulfate 6-O-sulfotransferase having different
12
13 specificities for hexuronic acid adjacent to the targeted N-sulfoglucosamine. *J Biol Chem* **2000**,
14
15 *275* (4), 2859-68.
16
17
18 30. Liu, R.; Liu, J., Enzymatic placement of 6-O-sulfo groups in heparan sulfate.
19
20 *Biochemistry* **2011**, *50* (20), 4382-91.
21
22
23 31. Jemth, P.; Smeds, E.; Do, A. T.; Habuchi, H.; Kimata, K.; Lindahl, U.; Kusche-
24
25 Gullberg, M., Oligosaccharide library-based assessment of heparan sulfate 6-O-sulfotransferase
26
27 substrate specificity. *J Biol Chem* **2003**, *278* (27), 24371-6.
28
29
30
31 32. Xu, Y.; Moon, A. F.; Xu, S.; Krahn, J. M.; Liu, J.; Pedersen, L. C., Structure Based
32
33 Substrate Specificity Analysis of Heparan Sulfate 6-O-Sulfotransferases. *ACS Chem Biol* **2017**,
34
35 *12* (1), 73-82.
36
37
38 33. Thieker, D. F.; Xu, Y.; Chapla, D.; Nora, C.; Qiu, H.; Felix, T.; Wang, L.; Moremen,
39
40 K. W.; Liu, J.; Esko, J. D.; Woods, R. J., Downstream Products are Potent Inhibitors of the
41
42 Heparan Sulfate 2-O-Sulfotransferase. *Sci Rep* **2018**, *8* (1), 11832.
43
44
45
46 34. Liu, C.; Sheng, J.; Krahn, J. M.; Perera, L.; Xu, Y.; Hsieh, P. H.; Dou, W.; Liu, J.;
47
48 Pedersen, L. C., Molecular mechanism of substrate specificity for heparan sulfate 2-O-
49
50 sulfotransferase. *J Biol Chem* **2014**, *289* (19), 13407-18.
51
52
53
54
55
56
57
58
59
60

- 1
2
3
4 35. Xu, D.; Song, D.; Pedersen, L. C.; Liu, J., Mutational study of heparan sulfate 2-O-
5
6 sulfotransferase and chondroitin sulfate 2-O-sulfotransferase. *J Biol Chem* **2007**, *282* (11), 8356-
7
8 67.
9
10
11 36. Tvaroška, I.; Kožár, T., Theoretical studies on the conformation of saccharides: Part VI.
12
13 Influence of the pyranoid ring shape on the conformational properties of the glycosidic linkage
14
15 and on the magnitude of the exoanomeric effect. *Journal of Molecular Structure: THEOCHEM*
16
17 **1985**, *123* (1), 141-154.
18
19
20
21 37. Berglund, J.; Angles d'Ortoli, T.; Vilaplana, F.; Widmalm, G.; Bergenstrahle-Wohlert,
22
23 M.; Lawoko, M.; Henriksson, G.; Lindstrom, M.; Wohlert, J., A molecular dynamics study of
24
25 the effect of glycosidic linkage type in the hemicellulose backbone on the molecular chain
26
27 flexibility. *Plant J* **2016**, *88* (1), 56-70.
28
29
30
31 38. Plazinski, W.; Lonardi, A.; Hunenberger, P. H., Revision of the GROMOS
32
33 56A6(CARBO) force field: Improving the description of ring-conformational equilibria in
34
35 hexopyranose-based carbohydrates chains. *J Comput Chem* **2016**, *37* (3), 354-65.
36
37
38
39 39. Hsieh, P. H.; Thieker, D. F.; Guerrini, M.; Woods, R. J.; Liu, J., Uncovering the
40
41 Relationship between Sulphation Patterns and Conformation of Iduronic Acid in Heparan
42
43 Sulphate. *Sci Rep* **2016**, *6*, 29602.
44
45
46 40. Spiwok, V.; Kralova, B.; Tvaroska, I., Modelling of beta-D-glucopyranose ring
47
48 distortion in different force fields: a metadynamics study. *Carbohydr Res* **2010**, *345* (4), 530-7.
49
50
51
52
53
54
55
56
57
58
59
60

- 1
2
3
4 41. Marforio, T. D.; Giacinto, P.; Bottoni, A.; Calvaresi, M., Computational Evidence for
5
6 the Catalytic Mechanism of Tyrosylprotein Sulfotransferases: A Density Functional Theory
7
8 Investigation. *Biochemistry* **2015**, *54* (28), 4404-4410.
9
10
11 42. Kadam, R. U.; Garg, D.; Schwartz, J.; Visini, R.; Sattler, M.; Stocker, A.; Darbre, T.;
12
13 Reymond, J. L., CH- π "T-shape" interaction with histidine explains binding of aromatic
14
15 galactosides to *Pseudomonas aeruginosa* lectin LecA. *ACS Chem Biol* **2013**, *8* (9), 1925-30.
16
17
18 43. Hudson, K. L.; Bartlett, G. J.; Diehl, R. C.; Agirre, J.; Gallagher, T.; Kiessling, L. L.;
19
20 Woolfson, D. N., Carbohydrate-Aromatic Interactions in Proteins. *J Am Chem Soc* **2015**, *137*
21
22 (48), 15152-60.
23
24
25 44. Stankovic, I. M.; Blagojevic Filipovic, J. P.; Zaric, S. D., Carbohydrate - Protein
26
27 aromatic ring interactions beyond CH/ π interactions: A Protein Data Bank survey and quantum
28
29 chemical calculations. *Int J Biol Macromol* **2020**, *157*, 1-9.
30
31
32 45. Montalvillo-Jimenez, L.; Santana, A. G.; Corzana, F.; Jimenez-Oses, G.; Jimenez-
33
34 Barbero, J.; Gomez, A. M.; Asensio, J. L., Impact of Aromatic Stacking on Glycoside
35
36 Reactivity: Balancing CH/ π and Cation/ π Interactions for the Stabilization of Glycosyl-
37
38 Oxocarbenium Ions. *J Am Chem Soc* **2019**, *141* (34), 13372-13384.
39
40
41 46. Kakuta, Y.; Sueyoshi, T.; Negishi, M.; Pedersen, L. C., Crystal structure of the
42
43 sulfotransferase domain of human heparan sulfate N-deacetylase/ N-sulfotransferase 1. *J Biol*
44
45 *Chem* **1999**, *274* (16), 10673-6.
46
47
48
49
50
51
52
53
54
55
56
57
58
59
60

- 1
2
3
4 47. Huntley, J. J.; Fast, W.; Benkovic, S. J.; Wright, P. E.; Dyson, H. J., Role of a solvent-
5
6 exposed tryptophan in the recognition and binding of antibiotic substrates for a metallo-beta-
7
8 lactamase. *Protein Sci* **2003**, *12* (7), 1368-75.
9
10
11 48. Tobola, F.; Lelimosin, M.; Varrot, A.; Gillon, E.; Darnhofer, B.; Blixt, O.; Birner-
12
13 Gruenberger, R.; Imberty, A.; Wiltschi, B., Effect of Noncanonical Amino Acids on Protein-
14
15 Carbohydrate Interactions: Structure, Dynamics, and Carbohydrate Affinity of a Lectin
16
17 Engineered with Fluorinated Tryptophan Analogs. *ACS Chem Biol* **2018**, *13* (8), 2211-2219.
18
19
20 49. Mueller, J. W.; Idkowiak, J.; Gesteira, T. F.; Vallet, C.; Hardman, R.; van den Boom,
21
22 J.; Dhir, V.; Knauer, S. K.; Rosta, E.; Arlt, W., Human DHEA sulfation requires direct
23
24 interaction between PAPS synthase 2 and DHEA sulfotransferase SULT2A1. *J Biol Chem* **2018**,
25
26 *293* (25), 9724-9735.
27
28
29 50. Foster, P. A.; Mueller, J. W., SULFATION PATHWAYS: Insights into steroid sulfation
30
31 and desulfation pathways. *J Mol Endocrinol* **2018**, *61* (2), T271-t283.
32
33
34 51. Gray, H. B.; Winkler, J. R., Hole hopping through tyrosine/tryptophan chains protects
35
36 proteins from oxidative damage. *Proc Natl Acad Sci U S A* **2015**, *112* (35), 10920-5.
37
38
39 52. Barducci, A.; Bonomi, M.; Parrinello, M., Metadynamics. *WIREs Computational*
40
41 *Molecular Science* **2011**, *1* (5), 826-843.
42
43
44 53. Barducci, A.; Bonomi, M.; Parrinello, M., Linking well-tempered metadynamics
45
46 simulations with experiments. *Biophys J* **2010**, *98* (9), L44-L46.
47
48
49 54. Tornberg, J.; Sykiotis, G. P.; Keefe, K.; Plummer, L.; Hoang, X.; Hall, J. E.; Quinton,
50
51 R.; Seminara, S. B.; Hughes, V.; Van Vliet, G.; Van Uum, S.; Crowley, W. F.; Habuchi, H.;
52
53
54
55
56
57
58
59
60

1
2
3
4 Kimata, K.; Pitteloud, N.; Bülow, H. E., Heparan sulfate 6-O-sulfotransferase 1, a gene involved
5
6 in extracellular sugar modifications, is mutated in patients with idiopathic hypogonadotropic
7
8 hypogonadism. *Proceedings of the National Academy of Sciences of the United States of*
9
10 *America* **2011**, *108* (28), 11524-11529.

11
12
13 55. Wagner, J. R.; Sorensen, J.; Hensley, N.; Wong, C.; Zhu, C.; Perison, T.; Amaro, R.
14
15 E., POVME 3.0: Software for Mapping Binding Pocket Flexibility. *J Chem Theory Comput*
16
17 **2017**, *13* (9), 4584-4592.

18
19
20 56. Jurrus, E.; Engel, D.; Star, K.; Monson, K.; Brandi, J.; Felberg, L. E.; Brookes, D. H.;
21
22 Wilson, L.; Chen, J.; Liles, K.; Chun, M.; Li, P.; Gohara, D. W.; Dolinsky, T.; Konecny, R.;
23
24 Koes, D. R.; Nielsen, J. E.; Head-Gordon, T.; Geng, W.; Krasny, R.; Wei, G. W.; Holst, M.
25
26 J.; McCammon, J. A.; Baker, N. A., Improvements to the APBS biomolecular solvation
27
28 software suite. *Protein Sci* **2018**, *27* (1), 112-128.

29
30
31 57. Record, M. T., Jr.; Ha, J. H.; Fisher, M. A., Analysis of equilibrium and kinetic
32
33 measurements to determine thermodynamic origins of stability and specificity and mechanism of
34
35 formation of site-specific complexes between proteins and helical DNA. *Methods Enzymol*
36
37 **1991**, *208*, 291-343.

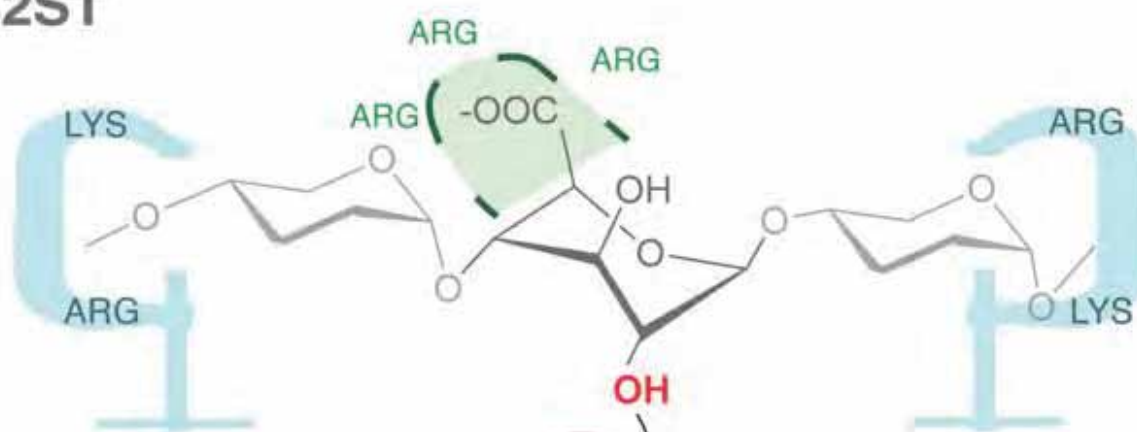
38
39
40 58. von Hippel, P. H., From "simple" DNA-protein interactions to the macromolecular
41
42 machines of gene expression. *Annu Rev Biophys Biomol Struct* **2007**, *36*, 79-105.

43
44
45 59. Kovacevic, B.; Baric, D.; Babic, D.; Bilic, L.; Hanzevacki, M.; Sandala, G. M.;
46
47 Radom, L.; Smith, D. M., Computational Tale of Two Enzymes: Glycerol Dehydration With or
48
49 Without B12. *J Am Chem Soc* **2018**, *140* (27), 8487-8496.
50
51
52
53
54
55
56
57
58
59
60

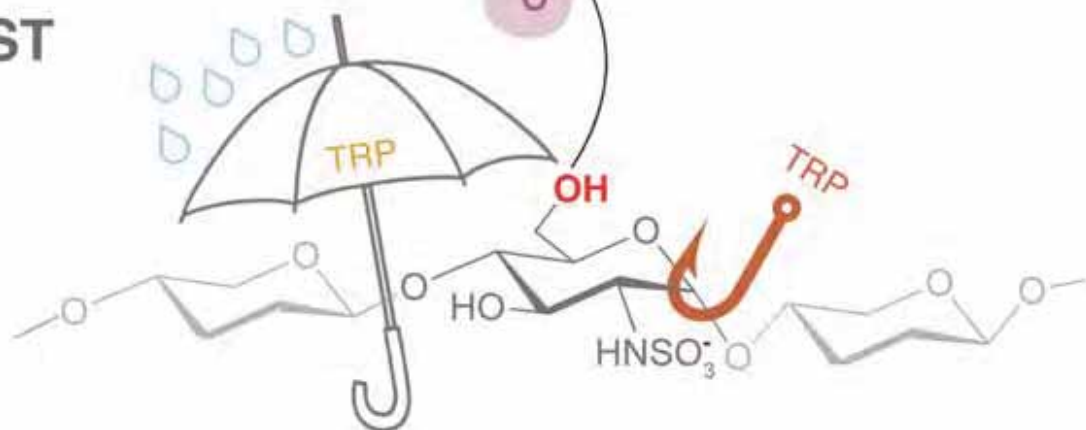
- 1
2
3
4 60. Nguyen, C. N.; Young, T. K.; Gilson, M. K., Grid inhomogeneous solvation theory:
5
6 hydration structure and thermodynamics of the miniature receptor cucurbit[7]uril. *J Chem Phys*
7
8 **2012**, *137*(4), 044101.
9
10
11 61. Van Agthoven, J. F.; Shams, H.; Cochran, F. V.; Alonso, J. L.; Kintzing, J. R.;
12
13 Garakani, K.; Adair, B. D.; Xiong, J. P.; Mofrad, M. R. K.; Cochran, J. R.; Arnaout, M. A.,
14
15 Structural Basis of the Differential Binding of Engineered Knottins to Integrins alphaVbeta3 and
16
17 alpha5beta1. *Structure* **2019**, *27*(9), 1443-1451 e6.
18
19
20
21 62. Pavlicek, J.; Coon, S. L.; Ganguly, S.; Weller, J. L.; Hassan, S. A.; Sackett, D. L.;
22
23 Klein, D. C., Evidence that proline focuses movement of the floppy loop of arylalkylamine N-
24
25 acetyltransferase (EC 2.3.1.87). *J Biol Chem* **2008**, *283*(21), 14552-8.
26
27
28
29 63. Yu, H.; Yan, Y.; Zhang, C.; Dalby, P. A., Two strategies to engineer flexible loops for
30
31 improved enzyme thermostability. *Sci Rep* **2017**, *7*, 41212.
32
33
34 64. Yu, H.; Zhao, Y.; Guo, C.; Gan, Y.; Huang, H., The role of proline substitutions within
35
36 flexible regions on thermostability of luciferase. *Biochim Biophys Acta* **2015**, *1854*(1), 65-72.
37
38
39 65. Cuneo, M. J.; Changela, A.; Warren, J. J.; Beese, L. S.; Hellinga, H. W., The crystal
40
41 structure of a thermophilic glucose binding protein reveals adaptations that interconvert mono
42
43 and di-saccharide binding sites. *J Mol Biol* **2006**, *362*(2), 259-70.
44
45
46 66. Cuneo, M. J.; Changela, A.; Beese, L. S.; Hellinga, H. W., Structural adaptations that
47
48 modulate monosaccharide, disaccharide, and trisaccharide specificities in periplasmic maltose-
49
50 binding proteins. *J Mol Biol* **2009**, *389*(1), 157-66.
51
52
53
54
55
56
57
58
59
60

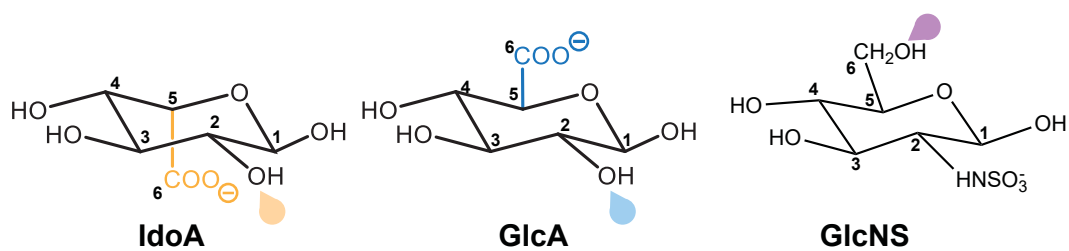
1
2
3
4 67. Shukla, S.; Bafna, K.; Gullett, C.; Myles, D. A. A.; Agarwal, P. K.; Cuneo, M. J.,
5
6 Differential Substrate Recognition by Maltose Binding Proteins Influenced by Structure and
7
8 Dynamics. *Biochemistry* **2018**, *57*(40), 5864-5876.
9
10

HS2ST

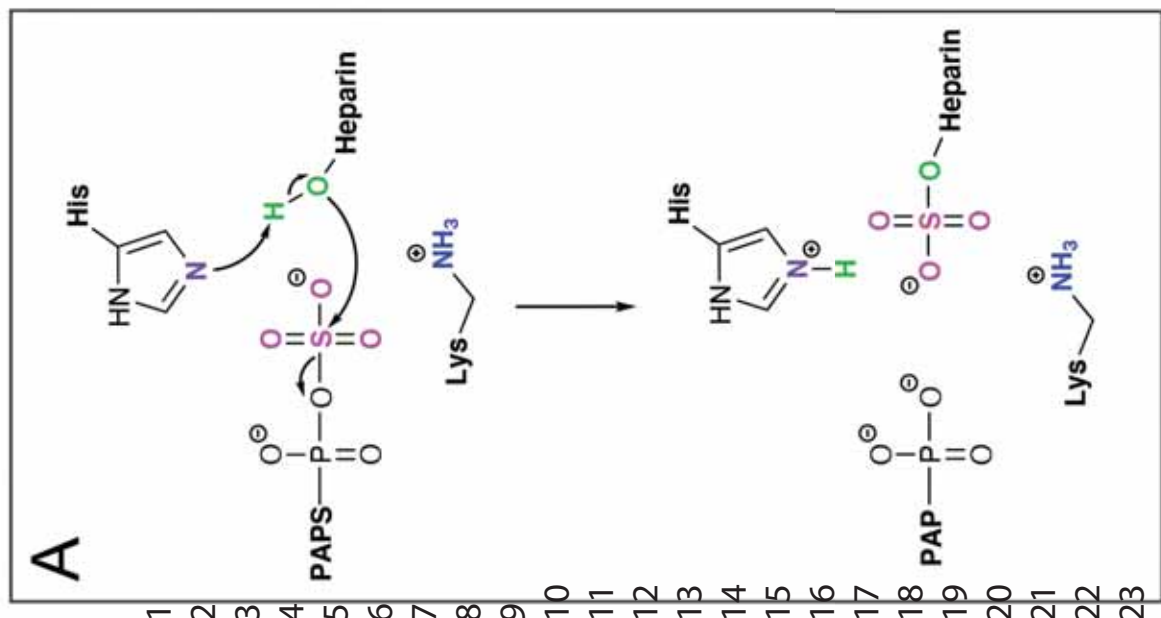


HS6ST

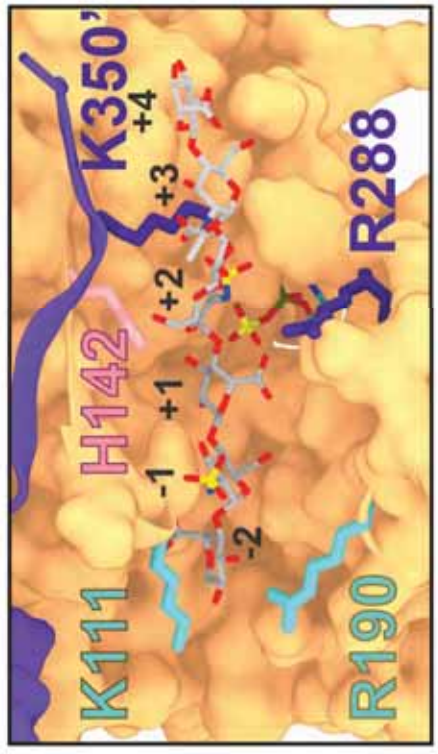
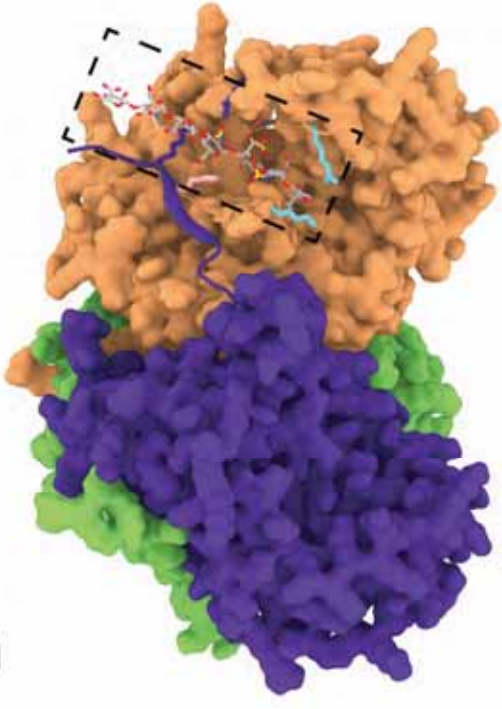




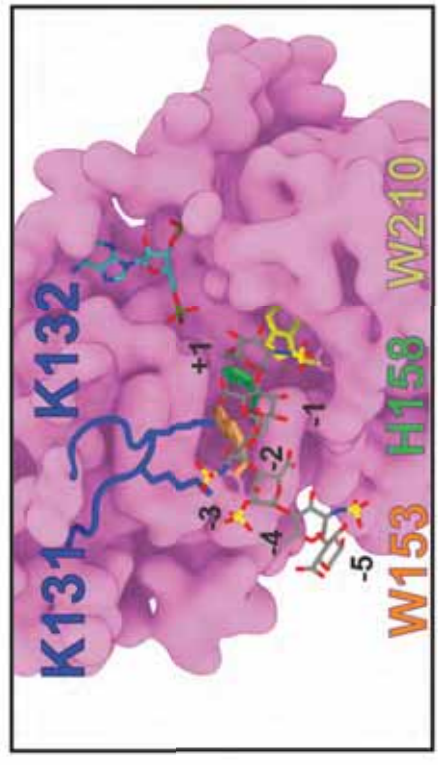
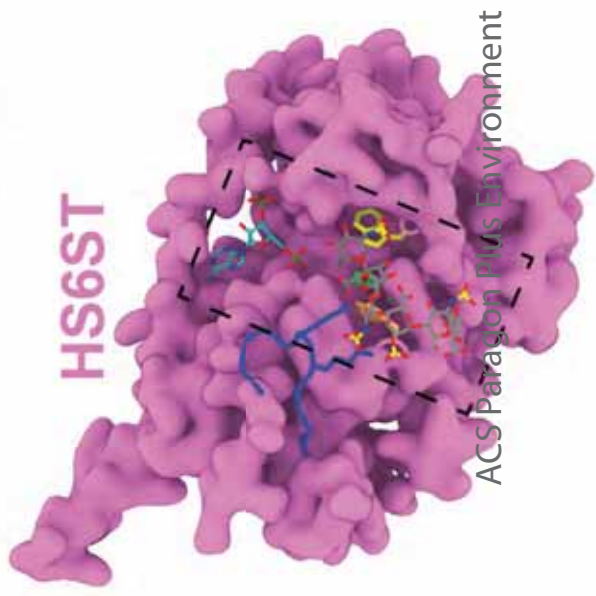
HGSST ACS Catalysis



B

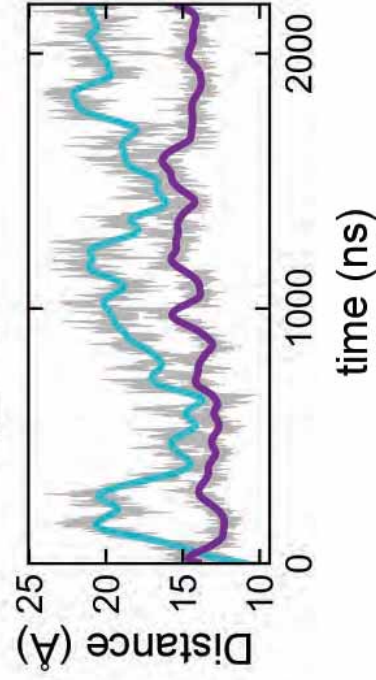


C

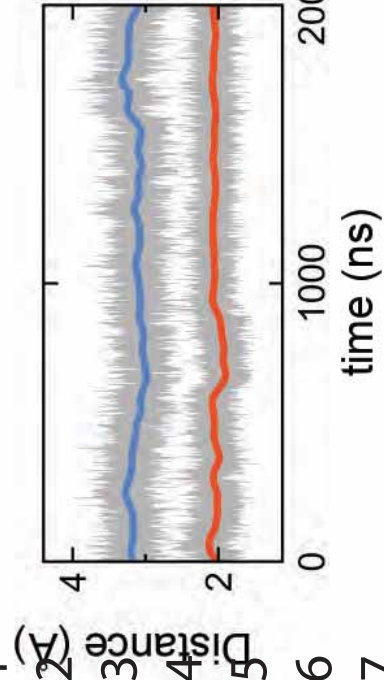


ACS Paragon Plus Environment

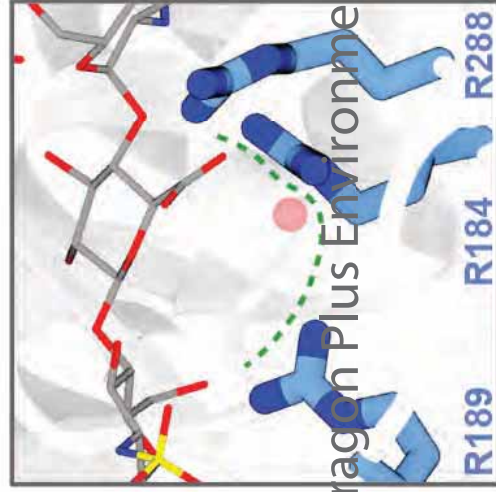
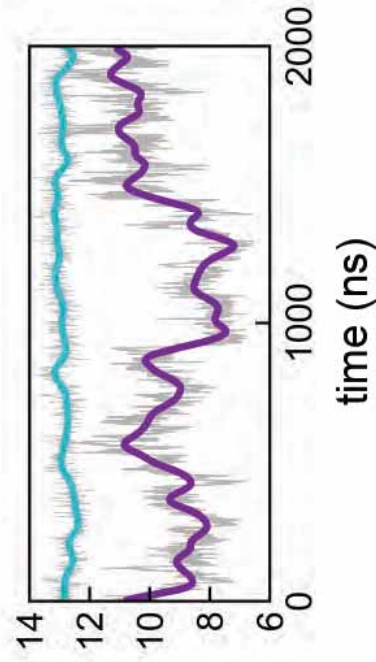
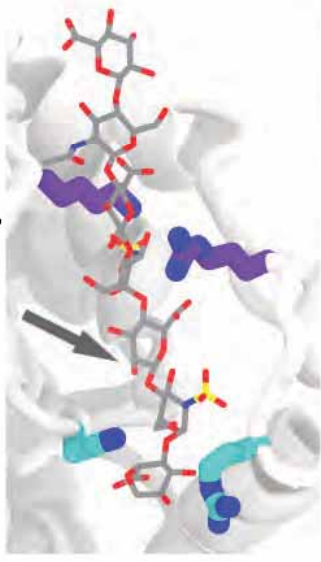
A Age 41 of 46 **HS2ST**^{apo}



B

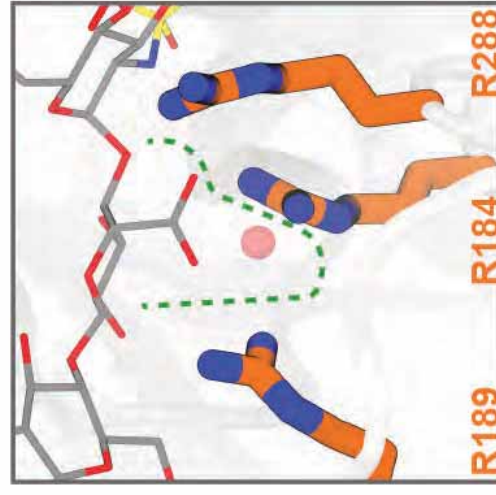
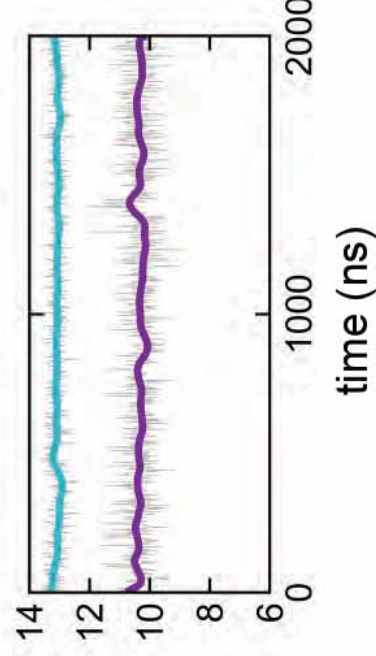
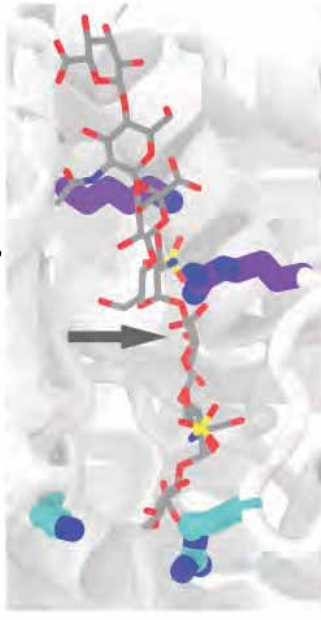


HS2ST^{apo} **G1cA**

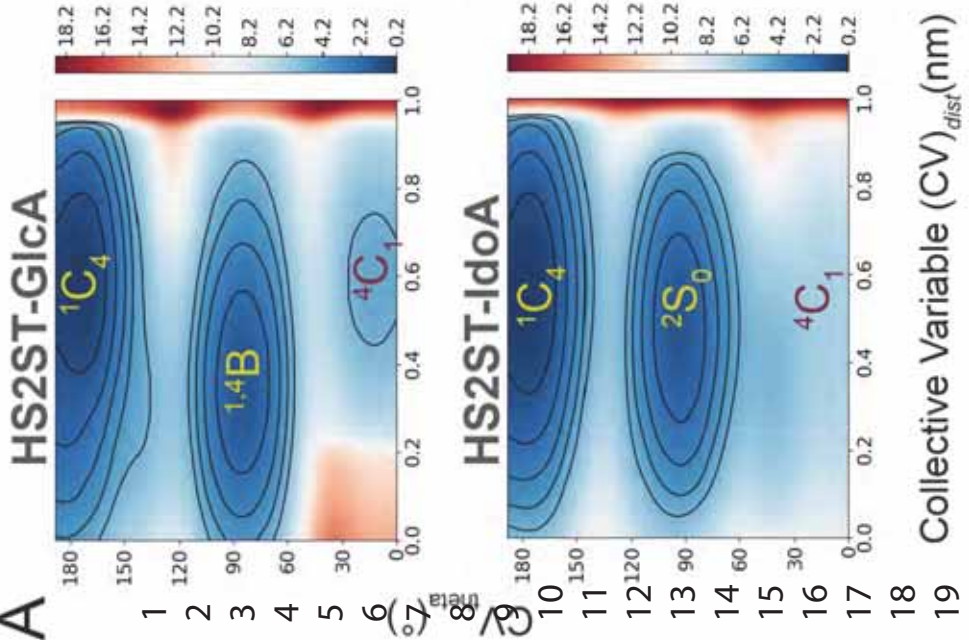


ACS Paragon Plus Environment

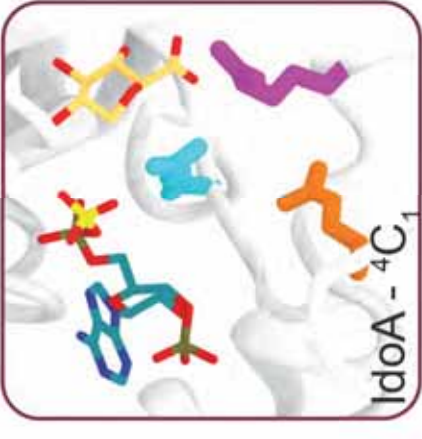
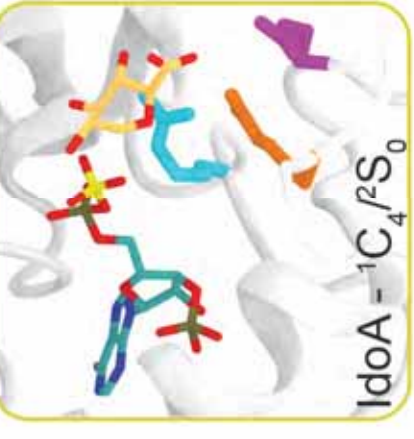
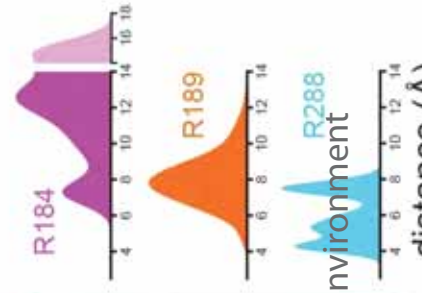
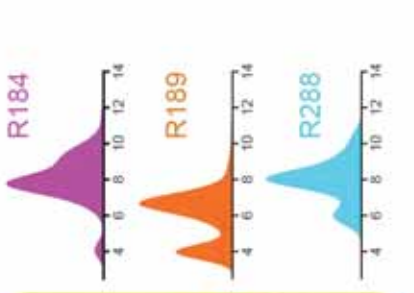
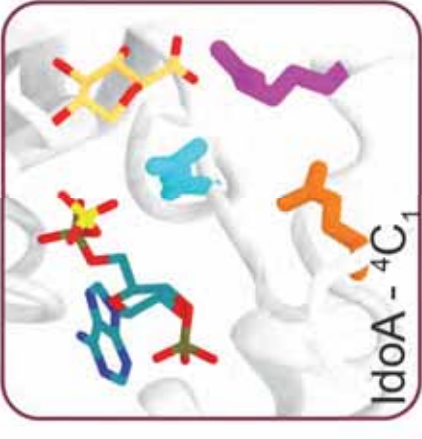
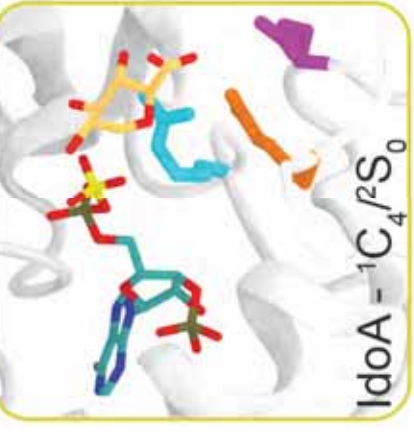
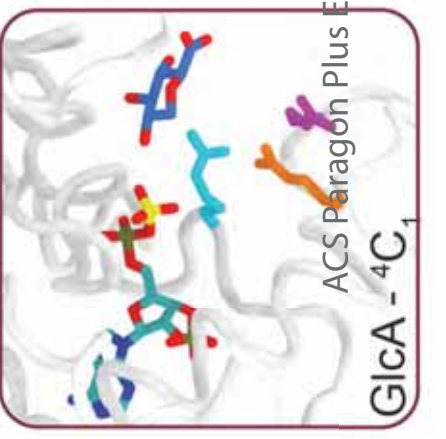
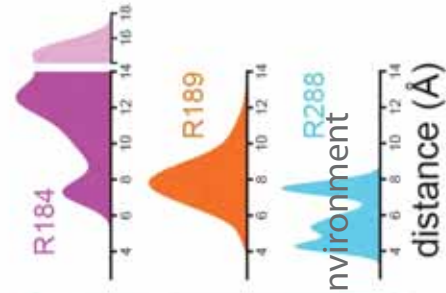
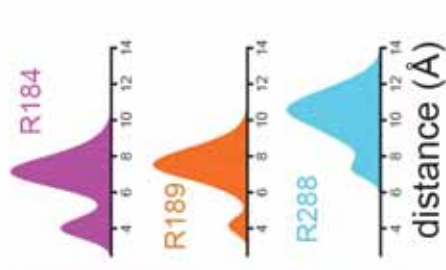
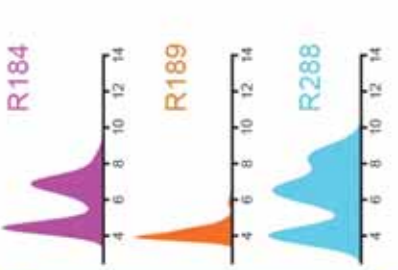
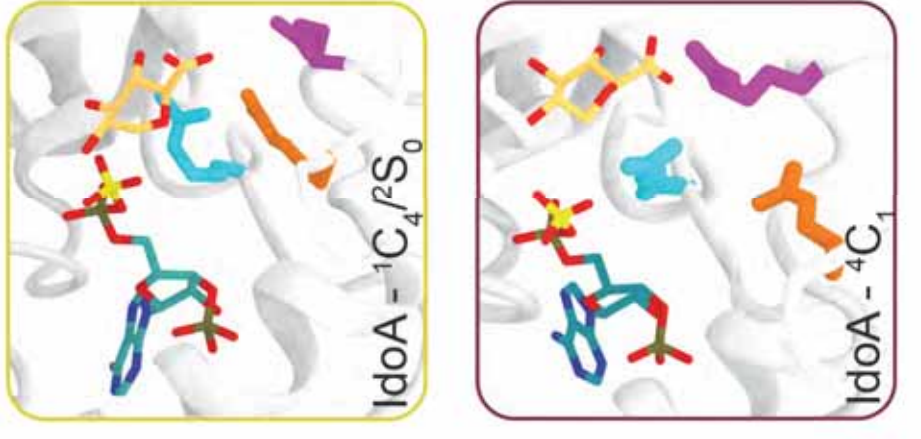
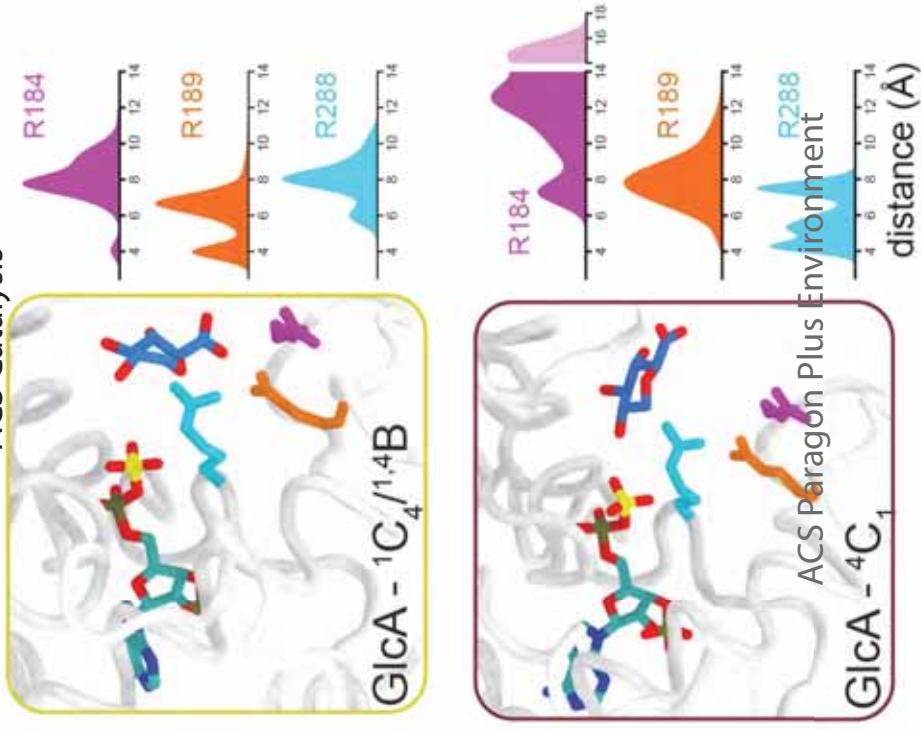
HS2ST-⁴C₁IdoA

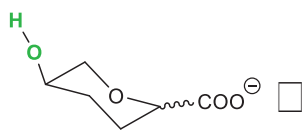
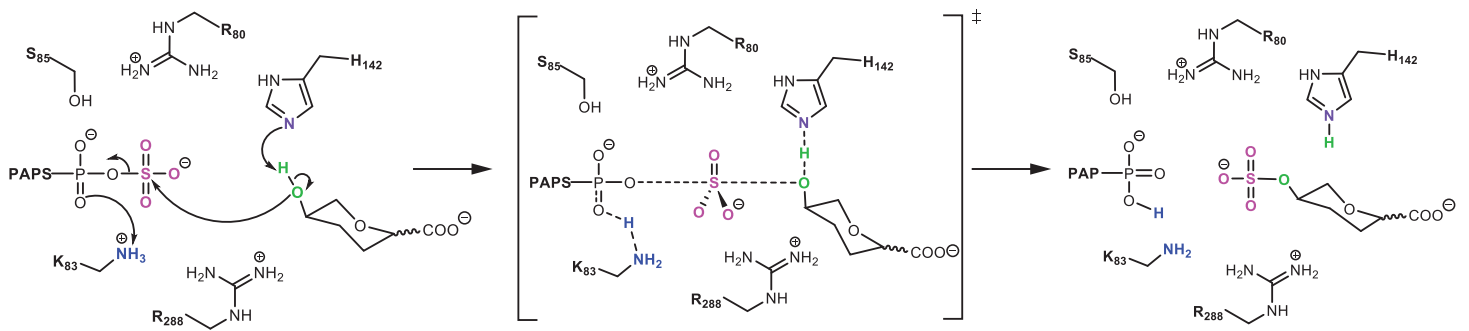


1
2
3
4
5
6
7
8
9
10
11
12
13
14
15
16
17
18

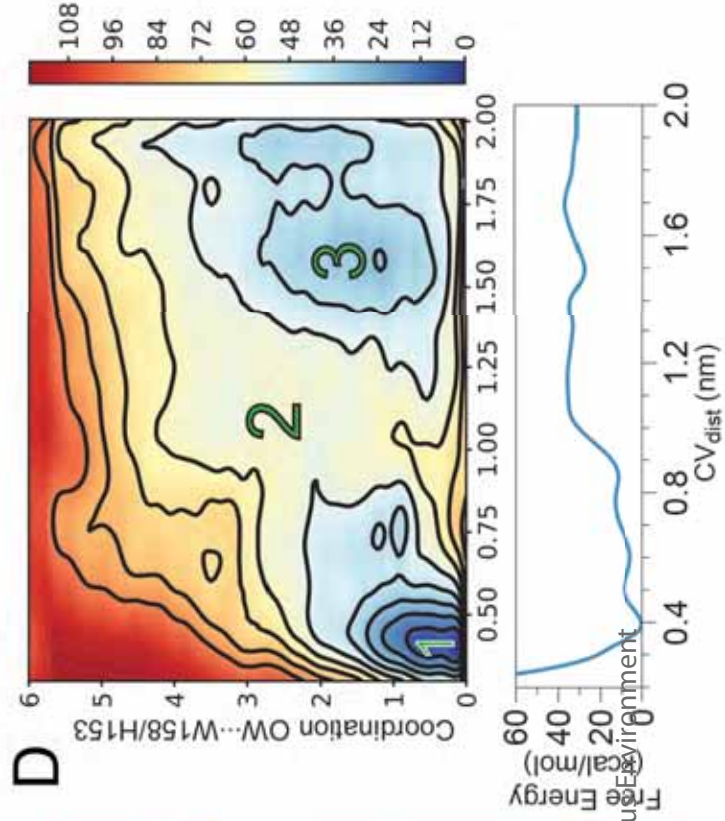
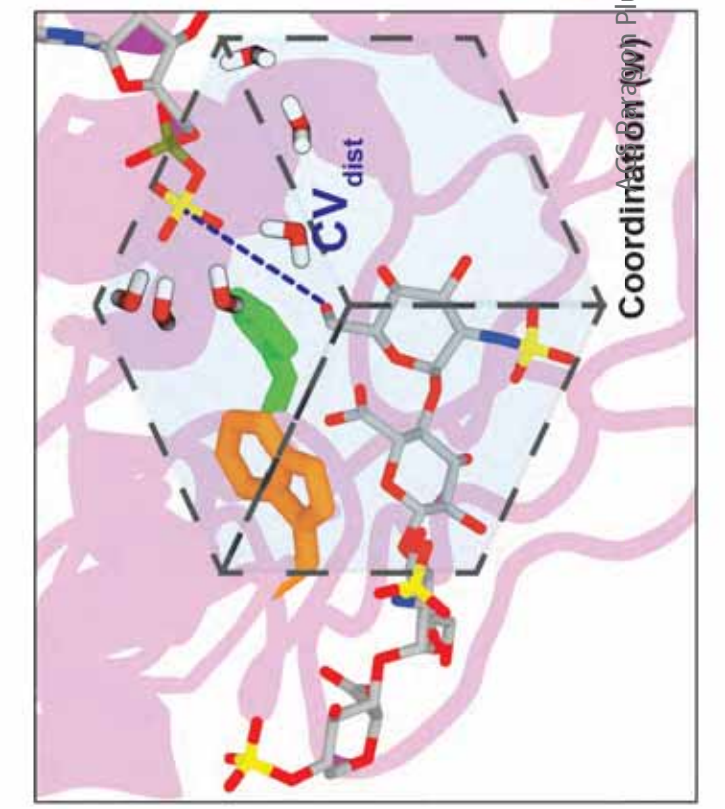
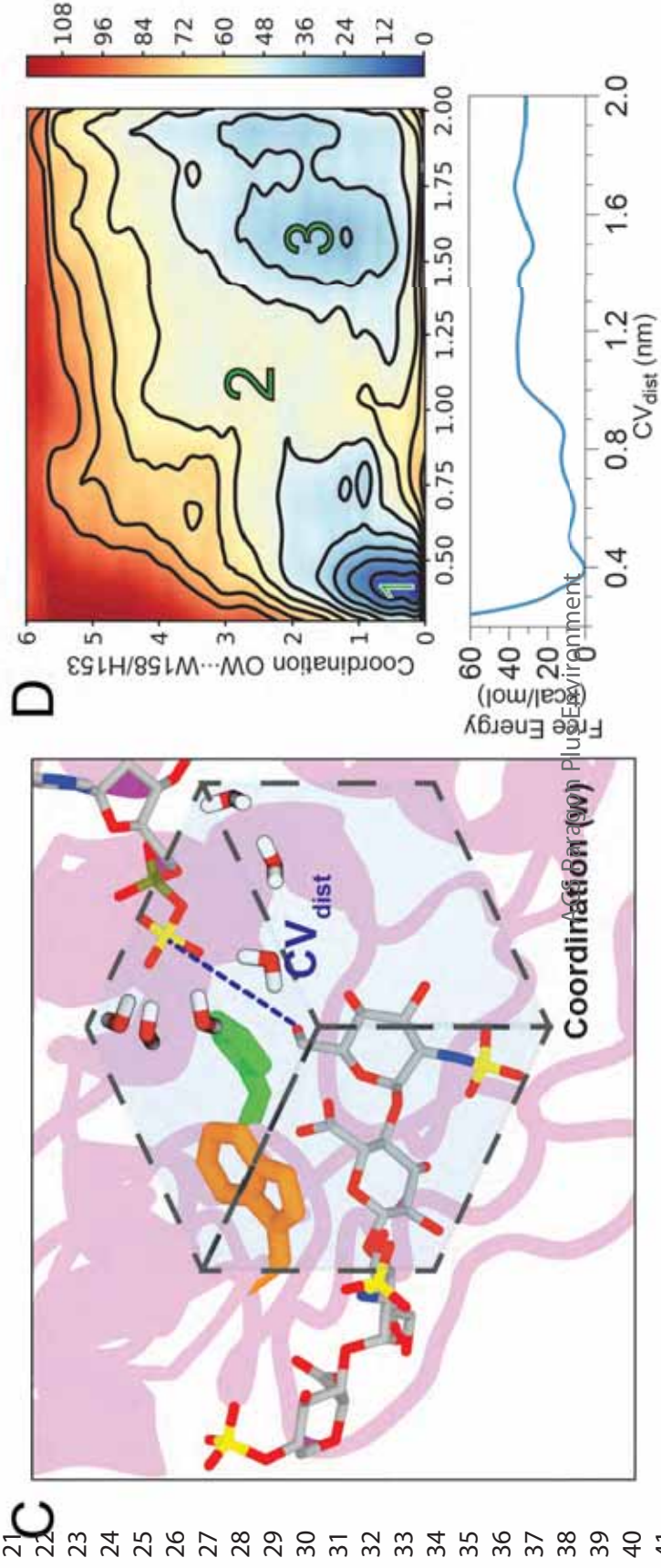
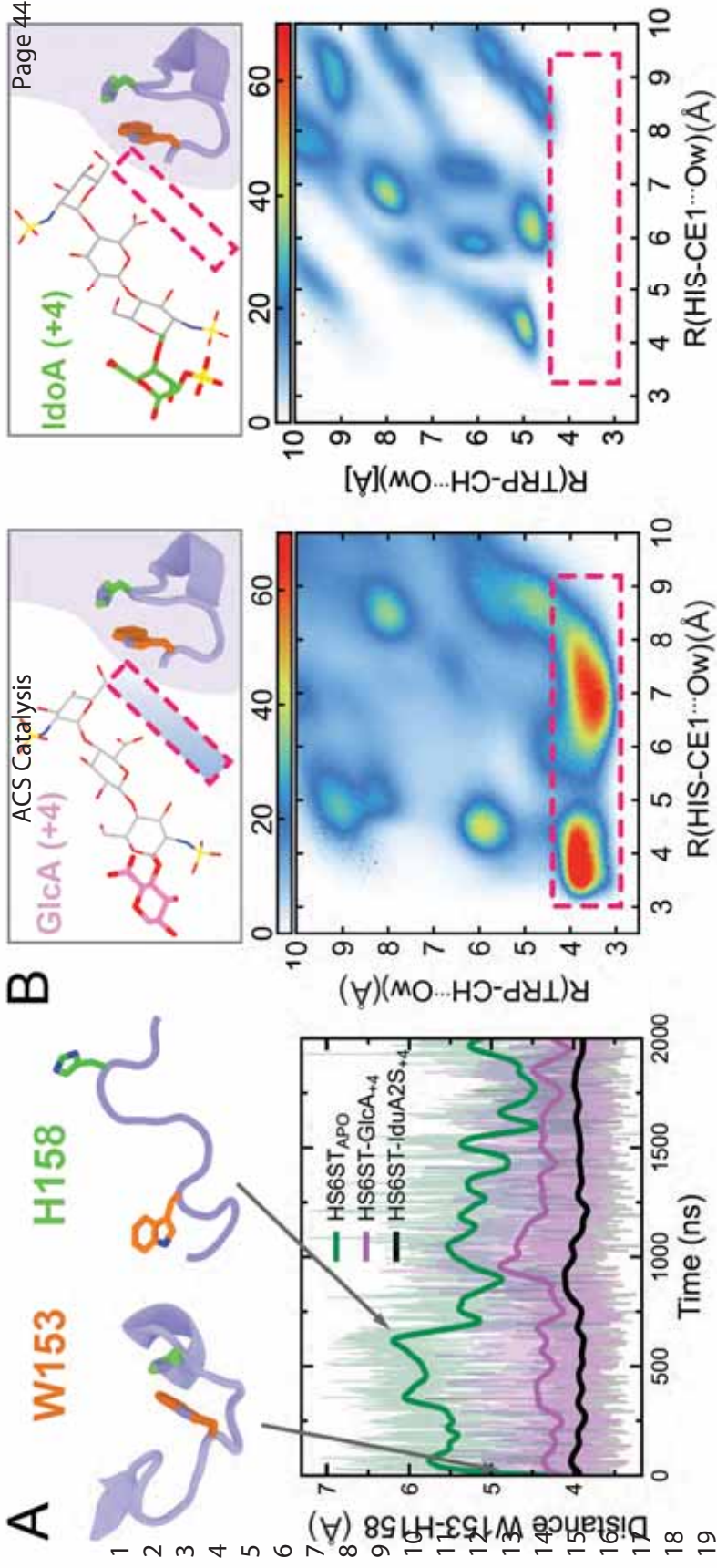


B

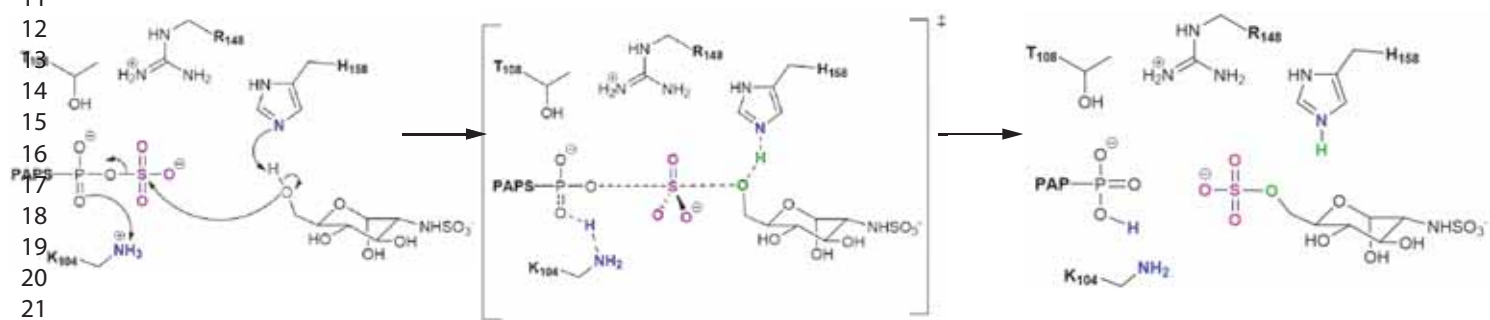




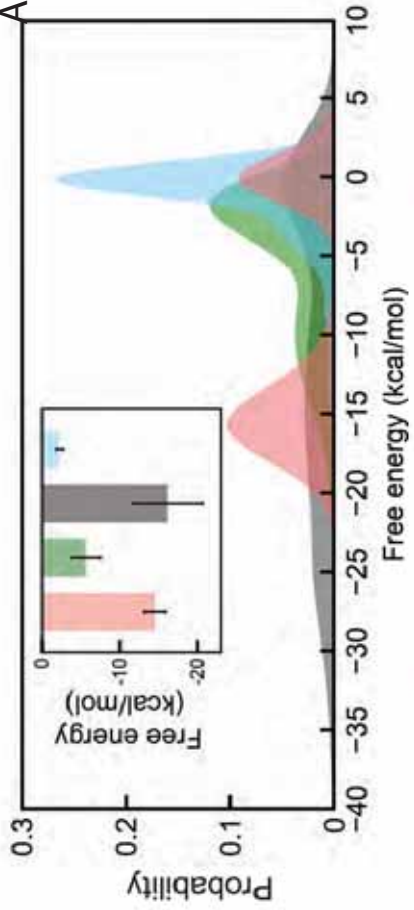
	$1 \rightarrow 4$ IdoA	$2 \rightarrow 5$ IdoA	$4 \rightarrow 1$ IdoA	$1 \rightarrow 4$ GlcA	$4 \rightarrow 1$ GlcA
ΔG^\ddagger	□□□□	□□□□	□3	2□□□	□□□□
ΔG	-□□□	□3□□	3□□	□□□	2□□



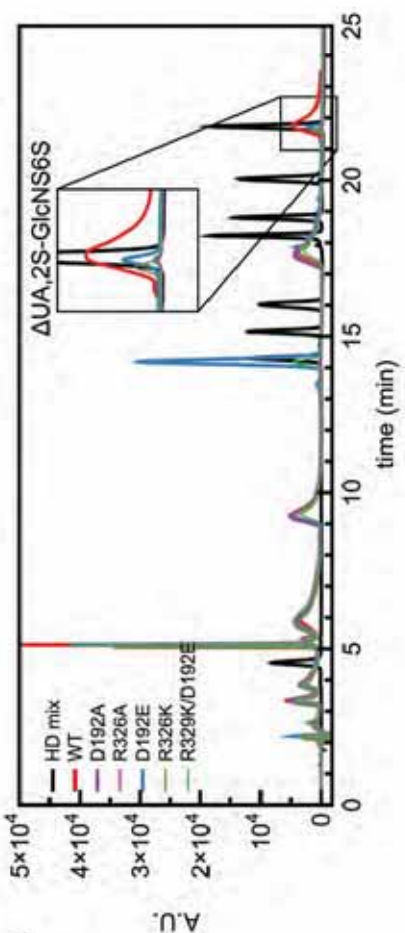
1
2
3
4
5
6
7
8
9
10
11
12
13
14
15
16
17
18
19
20
21
22
23
24
25
26
27
28
29
30
31
32
33
34
35
36
37
38
39
40
41

1
2
3
4
5
6
7
8
9
10
11
12
13
14
15
16
17
18
19
20
21
22
23
24
25
26
27
28
29
30
31
32
33
34
35
36
37
38
39
40
41
42
43
44
45
46
47
48
49
50
51
52
53
54
55
56
57
58
59
60

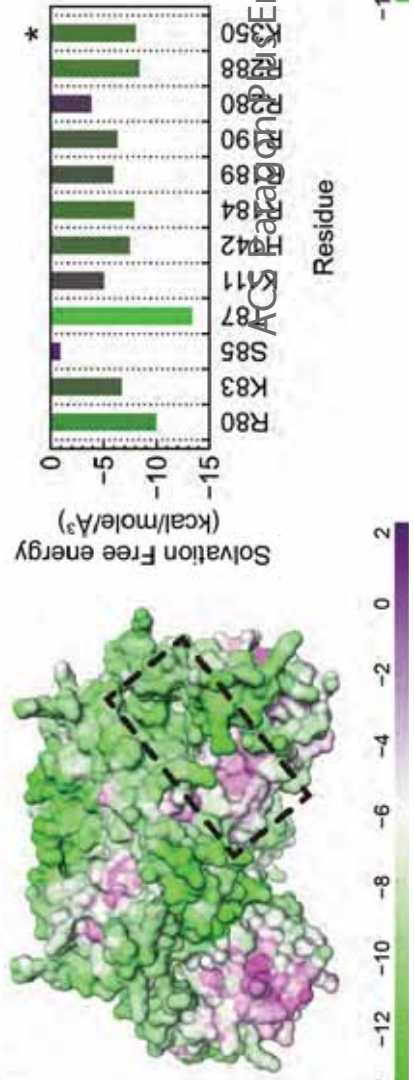
A



B



C



ACS Catalysis

Page 46 of 46

